1-1-2013

An Experimental Investigation of Diesel-Ignited Gasoline and Diesel-Ignited Methane Dual Fuel Concepts in a Single Cylinder Research Engine

Umang Dwivedi

An experimental investigation of diesel-ignited gasoline and diesel-ignited methane dual fuel concepts in a single cylinder research engine

By

Umang Dwivedi

A Thesis
Submitted to the Faculty of
Mississippi State University
in Partial Fulfillment of the Requirements
for the Degree of Master of Science
in Mechanical Engineering
in the Department of Mechanical Engineering

Mississippi State, Mississippi

August 2013

An experimental investigation of diesel-ignited gasoline and diesel-ignited methane dual fuel concepts in a single cylinder research engine

By

Umang Dwivedi

Approved:

Kalyan K. Srinivasan Associate Professor and Graduate Coordinator Mechanical Engineering (Major Professor)	Sundar R. Krishnan Assistant Professor Mechanical Engineering (Co-Major Professor)
Pedro J. Mago Associate Professor Mechanical Engineering (Committee Member)	Royce O. Bowden Interim Dean of the Bagley College of Engineering

Name: Umang Dwivedi

Date of Degree: August 17, 2013

Institution: Mississippi State University

Major Field: Mechanical Engineering

Major Professor: Dr. Kalyan Srinivasan

Title of Study: An experimental investigation of diesel-ignited gasoline and diesel-ignited methane dual fuel concepts in a single cylinder research engine

Pages in Study: 80

Candidate for Degree of Master of Science

Diesel-ignited gasoline and diesel-ignited methane dual fuel combustion experiments were performed in a single-cylinder research engine (SCRE), outfitted with a common-rail diesel injection system and a stand-alone engine controller. Gasoline was injected in the intake port using a port-fuel injector, whereas methane was fumigated into the intake manifold. The engine was operated at a constant speed of 1500 rev/min, a constant load of 5.2 bar IMEP, and a constant gasoline/methane energy substitution of 80%. Parameters such as diesel injection timing (SOI), diesel injection pressure, and boost pressure were varied to quantify their impact on engine performance and engine-out ISNOx, ISHC, ISCO, and smoke emissions. The change in combustion process from heterogeneous combustion to HCCI like combustion was also observed.

DEDICATION

I would like to dedicate this thesis to my mother Vani Dwivedi and to my sister Garima Dwivedi for their unconditional love, constant support and encouragement in all spheres of my life. A special dedication to my late father Mahendra Dwivedi, for being my greatest source of inspiration in life

ACKNOWLEDGEMENTS

I would like to acknowledge and express my sincere gratitude to my advisors Dr. Kalyan Srinivasan and Dr. Sundar Krishnan for their immense support, guidance and encouragement throughout my research. Their suggestions and instructions have been imperative to my professional growth. I would like to thank my colleagues Michael Gibson, Andrew Polk, Chad Carpenter, Scott Guerry, Mostafa Shameem, Pushkaraj Sakhare and Colin Mahony for always helping me out with my research and being there whenever I needed them. Special thanks to James A. Kizer for providing invaluable technical support with our emissions equipment. I would also like to thank Mr. Zach Rowland for his support throughout my research. Additional Thanks to my committee member Dr. Pedro J. Mago for his valuable comments and assistance.

I acknowledge the financial support provided by the Sustainable Energy Research Center and facilities support from the Center for Advanced Vehicular Systems at Mississippi State University.

TABLE OF CONTENTS

LIST OF TABLES

LIST OF FIGURES

NOMENCLATURE

η_{comb}	Combustion efficiency
AHRR	Apparent Heat Release Rate
A/F	Air-to-fuel ratio
BDC	Bottom Dead Center
BMEP	Brake Mean Effective Pressure
CA10-90	crank angle duration between the locations of 10% and 90% cumulative heat release
CA50	Crank angle corresponding to 50% of cumulative heat release
CA5	Crank angle corresponding to 5% of cumulative heat release
COV	Coefficient of Variation
DATDC	Degrees After Top Dead Center
DBTDC	Degrees Before Top Dead Center
EGR	Exhaust Gas Recirculation
FCE	Fuel Conversion Efficiency
FSN	Filter Smoke Number
ID	Ignition Delay
IFCE	Indicated Fuel Conversion Efficiency
IMEP	Indicated Mean Effective Pressure
LHV	Lower Heating Value

LTHR	Low Temperature Heat Release
MPRR	Maximum Pressure Rise Rate
PES	Percent Energy Substitution
PON	Pump Octane Number
Q_{HV}	Mass-averaged lower heating value (kJ/kg)
SADI	Stand Alone Direct Injection
SCRE	Single Cylinder Research Engine
SOC	Start of Combustion
SOI	Start of Injection of pilot fuel
TDC	Top Dead Center

Subscripts:

a	Air
main	Main fuel (Gasoline or Methane)
pilot	Pilot fuel(Diesel)
st	Stoichiometric
f	fuel
d	diesel

CHAPTER I

INTRODUCTION

Environmental, strategic, and economic factors are primary driving forces affecting the design and development of internal combustion (IC) engines. Alternatives to fossil-based fuels, including various biofuels [Karabektas et al. 2011, Agarwal 2007, Czerwinski 1994, Lin et. al 2007, Sayin 2010, Dorado 2003] , have been investigated. However, despite the promise of cleaner combustion with alternative fuels, high-volume production of renewable alternative fuels remains a formidable challenge. Therefore, fossil-based gasoline and diesel continue to be fuels of choice that power current IC engines. Also recent trends in fracking etc. have affected methane prices favorably and methane is being considered as a viable automobile fuel. Srinivasan et al. and Krishnan et al. have done many different analyses on diesel-methane dual fueling and have obtained some interesting results [Srinivasan et al. 2006, Krishnan 2004]. Propane is another such fuel which is slowly making its presence felt. Polk et al. explore low temperature combustion concept on a commercial heavy duty engine using propane [Polk et al. 2013].

The environmental effects of gasoline and diesel are well documented in the open literature [Fruin et. al 2001, Marshall et. al 2003, Mysliwiec et. al 2002, Rogge et. al 1993]. Traditionally, gasoline and diesel have powered spark ignition (SI) and compression ignition (CI) engines, respectively. In general, while gasoline-fueled SI engines suffer from poor part-load efficiencies and unburned hydrocarbon (HC) and carbon monoxide (CO) emissions, diesel-fueled CI engines suffer from high emissions of oxides of nitrogen (NOx) and particulate matter (PM) or soot. Recent improvements to CI engine combustion processes have attempted to leverage the premixed nature of traditional SI engine combustion and the throttle-less, direct-injection approach of traditional CI engines to achieve high-efficiency, clean combustion. Some of these strategies utilize the start of fuel injection (SOI) to control the start of combustion (SOC) and the separation between SOI and SOC to yield more premixing and very low engine-out NOx and PM emissions [Dec 2009]. These strategies have been termed low temperature combustion (LTC). While numerous researchers have investigated diesel-fueled LTC strategies to improve fuel conversion efficiencies and to reduce emissions from CI engines, some recent efforts [Kalghatgi et. al 2011, Hanson et. al 2009, Kalghatgi et. al 2009, Ciatti and Subramanian, 2011, Kalghatgi et. al 2013] have focused on operating CI engines on straight gasoline. For instance, recent research on partially premixed combustion strategies [Weall and Collings, 2009, Manente et. al 2009; Manente et. al 2010, Kalghatgi et. al 2007] shows that both heavy-duty and light-duty CI engines can be operated on gasoline at relatively high loads, while producing lower PM and NOx emissions compared to conventional diesel fuels. However, the major challenges with straight gasoline combustion in CI engines include higher CO and HC emissions at low loads and high pressure rise rates at high loads.

Some researchers have considered dual fuel combustion strategies [Inagaki et. al 2006], where gasoline-air mixtures are ignited using diesel pilots, and direct injection of gasoline-diesel blended fuels [Chao et. al 2013, Han et. al 2011, Han et. al 2012]. Of particular relevance to the present study is the gasoline-diesel dual fuel combustion process (also termed reactivity controlled compression ignition or RCCI), where premixed gasoline-air mixtures are ignited using appropriately timed diesel pilot sprays [Inaagaki et. al 2006, Kokjohn et. al 2009, Splitter et. al 2011, Kokjohn et. al 2011]. Gasoline, being highly volatile and more resistant to autoignition, is usually premixed with the intake air by fumigation or port injection. On the other hand, the more readily ignitable diesel fuel is injected directly into the cylinder to compression-ignite the gasoline fuel. The overall idea is that in-cylinder stratification of fuel reactivities between low-cetane gasoline and high-cetane diesel can be exploited to achieve control of the partially premixed combustion process. Low-cetane gasoline also results in longer ignition delay times compared to straight diesel operation, which ensures the separation of the diesel injection event from the overall combustion event, thus achieving LTC, and very low NOx and soot emissions.

Although diesel and gasoline have remained the fuels of choice for over a century recent advancements in fuel extraction technology, e.g. fracking, fuels such as methane and propane are re-emerging as economic and cleaner alternatives to gasoline and diesel. Thus investigation of methane as a prospective transportation fuel is relevant.

Classical dual fueling concept employs the fumigation of methane via the air intake manifold so that a good premixed charge-air mixture reaches the cylinder and the diesel pilot quantity is directly injected inside the cylinder near the end of compression stroke. Methane has a high octane rating (ON= 130) and high auto ignition temperatures making it difficult to ignite in a CI engine. Three distinct phases of combustion in a dual fuel engine using diesel (pilot fuel) and methane (primary fuel) have been identified by Karim, G. A., 2003. In the first phase energy is released from the combustion of diesel; in the second phase combustion of the methane surrounding diesel takes place; and in the third phase combustion of lean methane-air mixture takes place by flame propagation.

One of the primary reasons for recognizing methane as a future fuel is the ability to achieve reduced NOx and particulate matter (PM) relative to neat diesel operation. This is achieved by promoting lean burn [Doughty et al. 1992] which helps in achieving low local in cylinder temperatures, thereby reducing NOx emissions, and lowering knock tendencies. However, the fuel-lean combustion is accompanied by increased hydrocarbon (THC) and carbon monoxide (CO) emissions, resulting from bulk quenching and partial oxidation respectively [Papagiannakis and Hountalas, 2004]. Srinivasan et al 2006, Krishnan et al. 2004, employ advanced injection of small diesel pilots to ignite premixed Methane- air mixtures in the advanced low pilot ignited methane (ALPING) concept. This however resulted in very high unburned HC. Qi et al. 2006 and Srinivasan et al. 2007 used hot EGR and intake charge heating to achieve reduced HC along with low NOx and high efficiency benefits of ALPING combustion.

Another issue faced while trying to achieve the ignition of very lean methane mixtures is misfiring [Pitt 1984]. For successful ignition the energy release rate in early ignition phase must be greater than the energy losses incurred from the ignition kernel. Many concepts for achieving stable ignition via plot diesel charge, plasma jets, high energy spark and stratified charge/spark design have been proposed [Pitt 1984, Quader 1974, Anderson and Lim, 1985].

In this study the performance, emissions and combustion characteristics of diesel-gasoline and diesel-methane (methane surrogate) dual fueling have been investigated and compared using a single cylinder research engine. Ultra low sulfur diesel was used in both cases; a 93 PON gasoline was used for diesel-gasoline experiments, and pure methane (99.97% purity) was used for diesel-methane experiments in this thesis.

The primary objectives of this thesis are:

1. To investigate diesel-gasoline dual fueling at different injection timing, injection pressure and intake air conditions, at constant load (5.2 bar IMEP), speed (1500 rev/min) and 80 PES.
2. To investigate diesel-methane dual fueling at different injection timing, injection pressure and intake air conditions, at constant load (5.2 bar IMEP), speed (1500 rev/min) and 80 PES.
3. To present a brief comparison on the diesel-gasoline and diesel-methane studies over a range of injection timing case.

CHAPTER II

EXPERIMENTAL SETUP

A Single Cylinder Research Engine (SCRE) was used for conducting all experiments mentioned in this thesis. All the engine specifications are mentioned in Table 1. The engine was coupled to a 250HP AC regenerative engine dynamometer along with the interlock V controller, which provided the torque and speed measurements and control. The complete engine setup is shown in Figure 1.

Table 2.1 Engine Specifications

Engine Type	Rsi-130 DV 11 Single cylinder research engine, compression ignition
Bore x Stroke (mm x mm)	128 x 142
Connecting rod length (mm)	228
Displaced Volume (mm^3)	1.827×10^6
Compression ratio	17.1 : 1
Valve train system	4-valve, OHV
Diesel fuel injection system	CP3 Bosch common-rail
Injection system	Manifold port fuel injection (gasoline, methane)
Maximum speed	1900 rpm

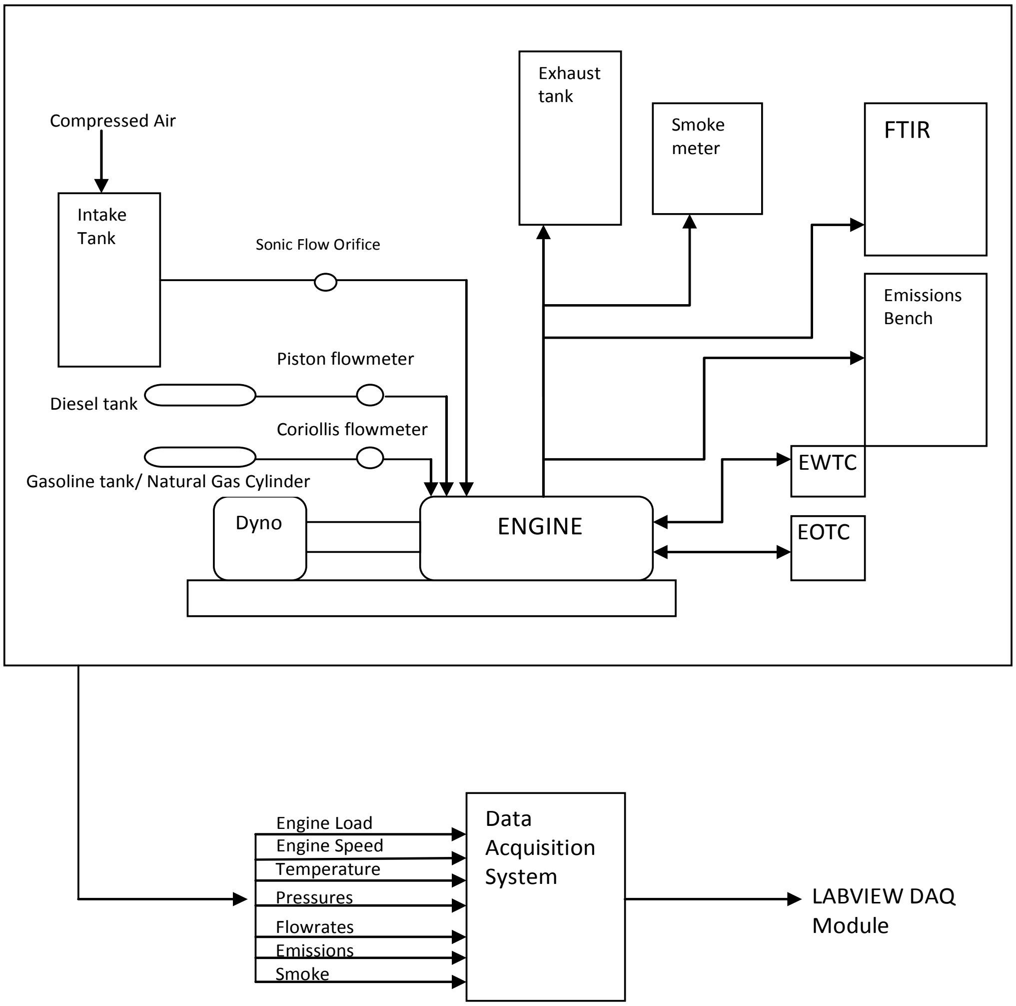

Figure 2.1 Experimental setup of the single cylinder engine

Gaseous and exhaust emissions were measured downstream of the exhaust manifold using an emissions sampling trolley and an integrated emissions bench (EGAS 2M) manufactured by Altech Environment S.A. All emissions were also verified using an AVL Fourier Transform Infra-red (FTIR) SESAM i60 FT. Smoke was measured in filter smoke number (FSN) units using an AVL 415S variable sampling smoke meter. The in-cylinder pressure (using a Kistler type 6052C pressure sensor and a Kistler 5010B type charge amplifier) and needle lift (Hall Effect sensor) sensors were phased with respect to crank angle using a BEI incremental shaft encoder with a resolution of 0.1 CAD (3600 pulses per revolution) coupled to the engine crankshaft. Apparent heat release rates (AHRR) were calculated from in-cylinder pressure data ensemble averaged over 100 cycles. The coolant and oil temperatures were maintained at 80ºC. An external air compressor and dryer were used to simulate intake charge boost. Intake air flow rates were measured using a calibrated sonic orifice by measuring the upstream pressure and temperature. Appropriate pressure ratios were maintained across the orifice to ensure choked flow at all times. Intake and exhaust temperatures, coolant temperatures and oil temperatures were measured using Omega Type-K thermocouples. A Max Machinery, Model 213 piston flow meter was used for measuring diesel (pilot) flow rate. A Micro Motion coriolis mass flow meter with 0.35% accuracy (of reading) was used to measure the gasoline/ Methane (secondary) flow rate. The 93 RON gasoline used in the testing program was injected into the intake manifold using a port fuel injector while direct injection of ULSD fuel was accomplished by a CP3 Bosch common rail pump and injector. The methane (methane surrogate) was injected via the air intake manifold. A Drivven stand-alone diesel injection (SADI) driver coupled with CALVIEW software was used to accomplish crank-resolved diesel and port-fueled gasoline injections. A needle valve was used to control the injection of methane.

Table 2.2 Fuel Properties

Parameter	No. 2 Diesel	Gasoline (93 PON)	Methane
LHV (MJ/kg)	42.5	42.1	50
Purity	N/A	N/A	99.97%
Laminar Burning Velocity*(cm/s)	N/A	N/A	40.5

*At 1 atm, 298 K and Φ=1

The engine performance parameters used in this work, such as Indicated fuel conversion efficiency, overall equivalence ratio (Φ), percent energy substitution (PES), ignition delay (ID_A), combustion efficiency (η_c) and Maximum pressure rise rate MPRR) are defined below.

$$PES = \frac{\dot{m}_{main} LHV_{main}}{\dot{m}_{pilot} LHV_{pilot} + \dot{m}_{main} LHV_{main}} \times 100\% \qquad (1)$$

$$\Phi = \frac{(A/F)_{st-tot}}{\frac{\dot{m}_a}{\dot{m}_{pilot} + \dot{m}_{main}}} \qquad (2)$$

$$ID_A = CA5 - SOI \qquad (3)$$

$$\eta_c = 1 - \frac{\sum_i x_i Q_{HV_i}}{[\dot{m}_f / (\dot{m}_a + \dot{m}_f)] Q_{HV}} \qquad (4)$$

$$MPRR = max.\left(\frac{dP}{d\theta}\right) \qquad (5)$$

$$IFCE = 100 \times \frac{IP}{(m_d Q_{LHVd} + m_{main} Q_{LHVmain})} \qquad (6)$$

In Equations 1 and 2, $\dot{m}$ refers to the mass flow rates of diesel (subscript pilot), gasoline/ methane fuel (subscript main), and air (subscript a), and *LHV* refers to the corresponding lower heating values of fuels. Stoichiometric air-fuel ratio $(A/F)_{st-tot}$ is defined as the stoichiometric air required for complete oxidation of both the pilot and the main fuels into CO_2 and H_2O. Therefore, $(A/F)_{st\text{-}tot}$ is dependent on the PES of gasoline. The start of combustion is defined as CA5, or the crank angle at which 5 percent of cumulative heat release occurs. In equation 4 [Heywood 1988] which represents combustion efficiency (η_c), x_i are the mass fractions of CO, H2, HC and particulates, Q_{HV_i} are the lower heating values of these species, and f and a denote fuel and air respectively. P refers to cylinder pressure and θ refers to the CAD. Equation 6 denotes indicated fuel conversion efficiency where m_d stands for mass of diesel fuel, m_{main} stands for mass of main fuel (gasoline or methane), Q_{LHVd} and Q_{LHVs} stand for lower heating values of diesel and main fuel respectively.

CHAPTER III

DIESEL-GASOLINE DUEL FUELING

3.1 Introduction

Diesel-ignited gasoline dual fuel combustion experiments [1] were performed in a single-cylinder research engine (SCRE), outfitted with a common-rail diesel injection system and a stand-alone diesel injection driver. Gasoline was injected in the intake port using a port-fuel injector. The engine was operated at a constant speed of 1500 rev/min, a constant load of 5.2 bar IMEP, and a constant gasoline energy substitution of 80%. Parameters such as diesel injection timing (SOI), diesel injection pressure, and boost pressure were varied to quantify their impact on engine performance and engine-out ISNOx, ISHC, ISCO, and smoke emissions. Advancing SOI from 30 DBTDC to 60 DBTDC reduced ISNOx from 14 g/kWhr to less than 0.1 g/kWhr; further advancement of SOI did not yield significant ISNOx reduction. A fundamental change was observed from heterogeneous combustion at 30 DBTDC to "premixed enough" combustion at 50-80 DBTDC and finally to well-mixed diesel-assisted gasoline HCCI-like combustion at 170 DBTDC. Smoke emissions were less than 0.1 FSN at all SOIs, while ISHC and ISCO were in the range of 8-20 g/kWhr, with the earliest SOIs yielding very high values. Indicated fuel conversion efficiencies were ~ 40-42.5%. An injection pressure sweep

[1] These results have been accepted for publication in the ASME Internal Combustion Engine Division conference, 2013

from 200 to 1300 bar at 50 DBTDC SOI showed that very low injection pressures lead to more heterogeneous combustion and higher ISNOx and ISCO emissions, while smoke and ISHC emissions remained unaffected. A boost pressure sweep from 1.1 to 1.8 bar at 50 DBTDC SOI showed very rapid combustion for the lowest boost conditions, leading to high pressure rise rates, higher ISNOx emissions, and lower ISCO emissions, while smoke and ISHC emissions remained unaffected by boost pressure variations.

3.2 Pilot Injection Timing: Performance and Emissions

The engine was operated at 5.2 bar IMEP, 1500 rev/min and 80 PES while diesel pilot injection timing was varied from 30 DBTDC to 170 DBTDC. The diesel injection pressure was maintained constant at 500 bar. The intake manifold pressure was set at 1.5 bar and no EGR was used.

3.2.1 Apparent Heat Release Rate and Cylinder Pressure

Figures 3.1 and 3.2 show the AHRR, cylinder pressure and needle lift profiles at different injection timings. As the injection timing is advanced from 30 to 170 DBTDC, the shape of the AHRR changes significantly. At 30 DBTDC, fuel injection begins at 330 CAD and ends at about 340 CAD. Also there are two distinct peaks and no significant low temperature heat release (LTHR) peak. Combustion is observed to start around 341 CAD, which indicates that the separation between the end of injection (EOI) and start of combustion (SOC) is very small, about 1 CAD. As a result, the diesel spray is stratified and retains its heterogeneity. This also indicates that the diesel is injected at high enough cylinder temperatures; as a result, there are no significant low temperature reactions that would warrant LTHR. Moreover, the occurrence of two AHRR peaks suggests that the first peak is likely due to the combustion of diesel and entrained gasoline and the second peak is likely due to mixing controlled burn of the lean (phi ~ 0.23) gasoline-air mixture. At 40 DBTDC, fuel injection begins at 320 CAD and ends around 330 CAD. The main combustion event starts around 342 CAD, which indicates that the separation between EOI and SOC is about 12 CAD. Additionally, a distinct LTHR peak is seen around 340 CAD, which is likely due to low temperature reactions leading to heat release from the high cetane diesel fuel. The two distinct peaks seen at 30 DBTDC are somewhat merged at 40 DBTDC. As the injection timing is advanced to 50 DBTDC, the separation between EOI, which is around 320 CAD and SOC, which is around 348 CAD, is 28 CAD. Clearly, the injection and combustion events are beginning to get increasingly separated. Also, the LTHR peak seen at 340 CAD at 40 DBTC SOI is seen at 50 DBTDC. The overall shape of the AHRR indicates predominantly a premixed burn. It is hypothesized that the early injection allows the injected diesel to attain a "premixed enough" state [Kalghatgi, G.T., et. al, 2010], which results in faster local burn rates while maintaining "slow enough" overall burn in the surrounding lean gasoline-air mixture as indicated by the smooth sinusoidal AHRR profile. As SOI is advanced further to 80 and 170 DBTDC, the AHRR peak magnitude increases, and is phased almost at TDC. Also, the LTHR magnitude and location is unchanged at 340 CAD. For instance, at 170 DBTC, the separation between injection and combustion is about 155 CAD. This indicates long residence times for diesel droplets to mix with the surrounding gasoline-air mixture, when the in-cylinder pressure and temperature are conducive to ignition around 355 CAD, combustion occurs instantaneously. This combustion is similar to diesel-assisted gasoline HCCI, which is characterized by high maximum pressure rise rates and short combustion durations. With increasing SOI advance, the state of the injected diesel fuel transitions from “premixed enough” to “well-mixed”. This “over mixing” results in a loss of the “heterogeneity” required to maintain combustion control. In other words, the window of SOIs between 50 - 80 DBTDC maintain the “premixed enough” state for the low cetane diesel fuel, which is required for overall combustion control.

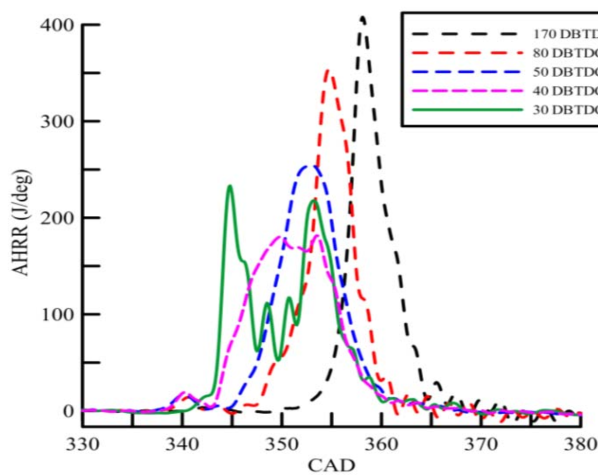

Figure 3.1 AHRR schedules at various injection timings at 5.2 bar IMEP, 80 PES, N= 1500 RPM, Pin = 1.5 bar

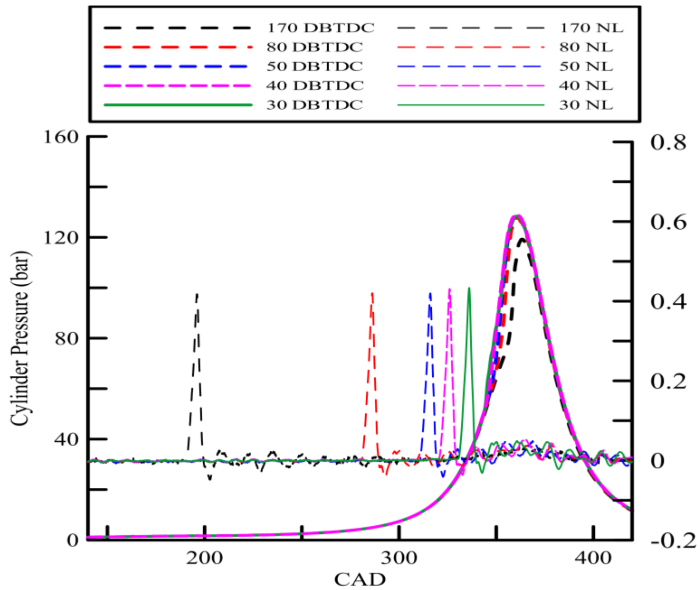

Figure 3.2 Cylinder pressure schedules and needle lift profiles at various injection timings at 5.2 bar IMEP, 80 PES, N= 1500 RPM, Pin = 1.5 bar

3.2.2 Ignition Delay, Maximum Pressure Rise Rate and Rate of Combustion

Figures 3.3 and 3.4 show ignition delay, MPRR, CA5, CA50 and CA10-90 trends over the range of SOIs from 30–170 DBTDC at 80% gasoline PES. Ignition delay increases with increasing injection advance from about 25 CAD at 30 DBTDC to 160 CAD at 170 DBTDC. With port-injected gasoline, the increase in ignition delay can be attributed primarily to increased residence times available for diesel to mix with the surrounding gasoline-air mixture; however, there seems to be a critical injection advance beyond which combustion transitions from RCCI to diesel-assisted HCCI – like combustion. To verify this, it is instructive to examine the nature of ignition delays, CA10-90 and CA50 at 50, 80 and 170 DBDTC injection timings. At 50 DBTDC, the ignition delay or time available for diesel premixing is about 38 CAD or 4.2ms, at 80 DBTDC, the ignition delay is about 70 CAD or 7.8ms and at 170 DBTDC, the ignition delay is about 162 CAD or 18ms. Also from Figure 5, the corresponding CA10-90 (combustion durations) are 8.3 CAD (0.92ms), 7.7 CAD (0.85ms) and 6.1 CAD (0.67ms), respectively. Additionally, the CA50s are also progressively retarded towards TDC, i.e. -8 DATDC, -6 DATDC and -2 DATDC, respectively. These data make for an interesting comparison since the overall equivalence ratio is maintained constant around 0.23 for the entire injection timing sweep.

As the injection timing is advanced from 50 DBTDC to 170 DBTDC, the time available for diesel premixing increases fourfold (from 4.2ms to 18ms), as a result, the diesel tends to get increasingly "well mixed" at advanced SOIs. The major consequence of this increased mixing is that the advantage of the difference between the ignition characteristics of the two fuels, diesel (CN~45) and gasoline (CN~26) ceases to assume any prominence since the combustion is now chemical kinetics dominated; therefore, there is lack of combustion control as indicated by increased MPRR, which is nearly 13 bar/CAD at 170 DBTDC. In contrast, at 50 DBTDC, the difference in ignition characteristics or chemical reactivity's between the two fuels can be used to control the overall combustion, i.e., it is possible to achieve faster local combustion rates, while maintaining a slower overall combustion rate. This is primarily due to the fact that some level of "stratification" is still retained, or in other words, the combustion is just "premixed enough" to keep the MPRR lower (approximately 8.5 bar/CAD) than that at 170 DBTDC injection timing. Therefore, the difference in reactivity's of the two fuels with extremely different (diesel, CN~45 and gasoline, CN~26) can be exploited only if the higher cetane fuel (in this case, diesel) is just "premixed enough." It must be noted that the effect of EGR, a significant variable that can affect the nature of RCCI combustion, was not investigated in this study. It may be possible to extend the range of injection timings where the benefits of RCCI combustion can be fully realized with aggressive amounts of cooled EGR.

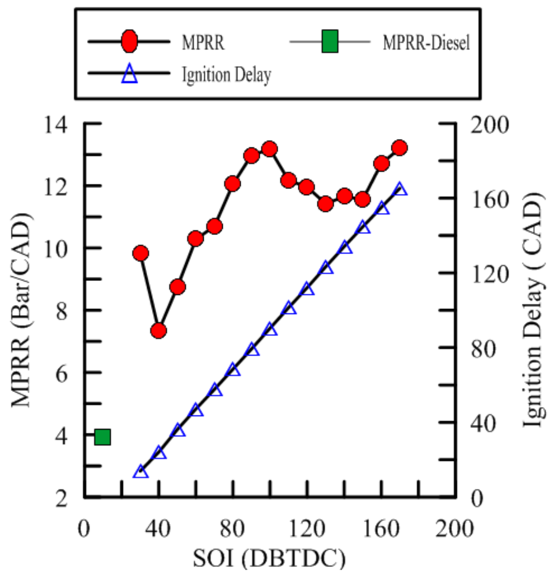

Figure 3.3 MPRR and Ignition delay at various injection timings at 5.2 bar IMEP, 80 PES, N= 1500 RPM, Pin = 1.5 bar

3.2.3 Fuel Conversion Efficiency and Combustion Efficiency

Figure 3.5 shows the indicated fuel conversion and combustion efficiencies between 30 and 170 DBTDC SOI at a constant load of 5.2 bar IMEP and 80% PES. Clearly, the combustion efficiency decreases with increasing injection advance, indicating that the HC and CO emissions are likely high at these injection timings. This is confirmed in Figure 7. Also, the IFCE decreases from 42.5% at 50 DBTDC to nearly 40% at 170 DBTDC. This decrease in IFCE can be attributed to the decreased combustion efficiencies at the advanced injection timings.

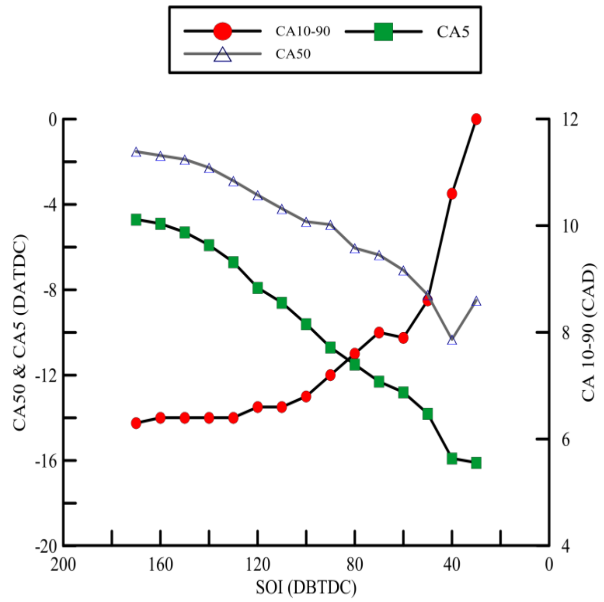

Figure 3.4 CA5, CA50 and CA10-90 at various injection timings at 5.2 bar IMEP, 80 PES, N= 1500 RPM, Pin = 1.5 bar

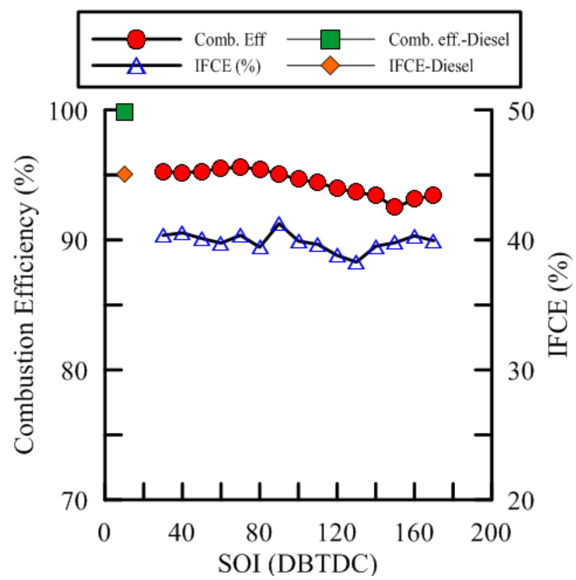

Figure 3.5 Combustion and Indicated Fuel Conversion efficiencies at various injection timings at 5.2 bar IMEP, 80 PES, N= 1500 RPM, Pin = 1.5 bar

3.2.4 Emissions

Figure 3.6 shows the ISCO and ISHC emissions trends between 30 and 170 DBTDC SOI at a constant load of 5.2 bar IMEP and 80% PES. ISHC and ISCO follow similar trends with injection advance. ISCO decreases from about 14 g/kWhr at 30 DBTDC to 8 g/kWhr at 80 DBTDC and then increases to 20 g/kWhr at 170 DBTDC. ISHC decreases from 10 g/kWhr at 30 DBTDC to about 9 g/kWhr at 60 DBTDC and then increases to nearly 14 g/kWhr at 170 DBTDC. To understand these trends, it is instructive to look at the AHRR curves in Fig. 2. From Fig. 2 it is seen that combustion is essentially complete at or before TDC for 30-80 DBTDC SOI. On further advance, say at 170DBTDC, combustion is slightly retarded away from TDC and is complete around 5 DATDC. With increasing injection advance diesel is injected into progressively less-dense gasoline-air mixtures. This indicates that the spray penetration is longer and the possibility of spray-wall or spray-piston interaction is higher. As a result, a significant amount of the injected diesel fuel can escape into cooler boundary layers and not participate in the ignition of the premixed gasoline-air mixture. Due to the unavailability of the more reactive diesel fuel, the combustion/oxidation of the lean premixed gasoline-air mixture may become increasingly impeded resulting in increased unburned and/or partially oxidized fuel that manifest as increased HC and CO emissions. As the injection timing is retarded, say at 80 DBTDC, the diesel spray encounters progressively denser mixtures; as a consequence, spray penetration lengths are shorter. This results in better stratification and greater availability of the high cetane diesel fuel to initiate combustion of the lean premixed gasoline-air mixture. Therefore, the ensuing HC and CO emissions are comparatively lower in magnitude. Now, with further injection retard, say at 30

DBTDC, the overall combustion rates are faster due to increased stratification of the diesel spray in the surrounding lean premixed gasoline-air mixture. This is evidenced by the combustion completing before TDC. After this, there is no more fuel energy to sustain the combustion process, as a result, during the expansion process; the burned gases are subject to rapid cooling. This cooling causes a drastic reduction in bulk in-cylinder temperatures, which freezes CO chemistry, thereby leading to high engine-out CO emissions.

The ISNOx and smoke emissions in Figure 3.7 show an interesting trend. On advancing the injection timing from 30 DBTDC to 40 DBTDC, the NOx emissions dramatically drop from 14 g/kWhr to 2 g/kWhr and further SOI advance reduces the NOx emissions down to near zero levels, while the smoke emissions remain unchanged throughout the injection timing sweep at less than 0.1 FSN. This dramatic NOx reduction is related to the increased residence times available for the diesel pilot to mix with the surrounding gasoline-air mixtures. This increased mixing with increased injection advance results in increasingly homogeneous in-cylinder mixtures, which in-turn results in low local temperatures, much below the thermal NOx formation threshold temperatures of 1900 K. Consequently, the NOx emissions are reduced to near-zero levels. The simultaneous reduction of NOx and smoke emissions is an indirect proof of the occurrence of low temperature combustion (LTC) under these conditions.

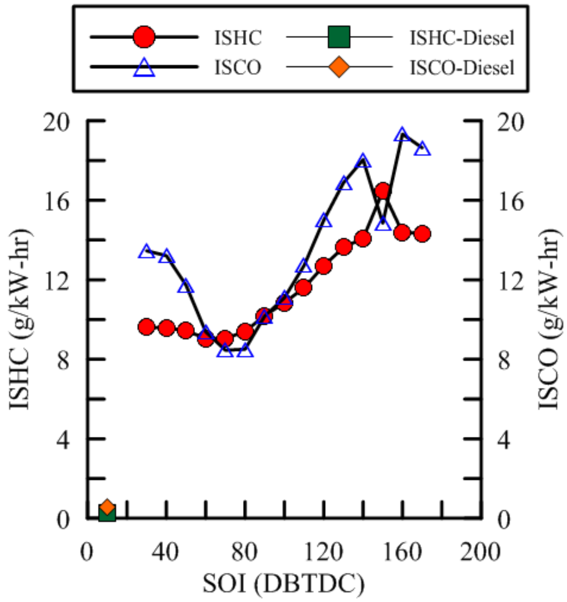

Figure 3.6 ISHC and ISCO emissions at various injection timings at 5.2 bar IMEP, 80 PES, N= 1500 RPM, Pin = 1.5 bar

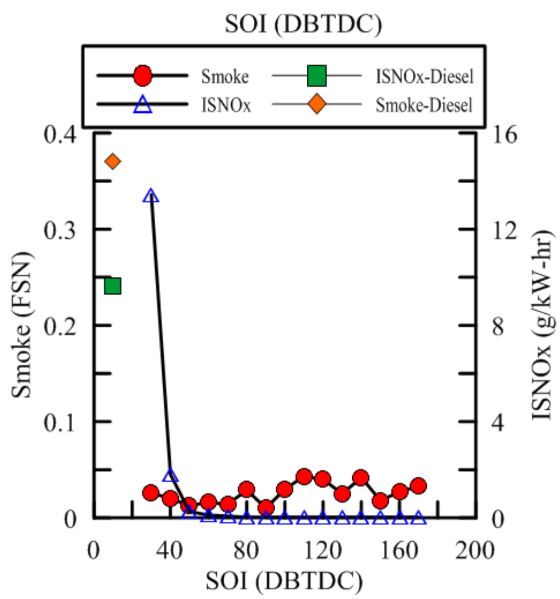

Figure 3.7 ISNOx and smoke emissions at various injection timings at 5.2 bar IMEP, 80 PES, N= 1500 RPM, Pin = 1.5 bar

3.3 Rail Pressure: Performance and Emissions

The engine was operated at 5.2 bar IMEP, 1500 rev/min and 80 PES at 50 DBTDC SOI and constant boost pressure of 1.5 bar while injection pressure was varied from 200 bar to 1300 bar.

3.3.1 Apparent Heat Release Rate and Cylinder Pressure

Figure 3.8 and 3.9 show the AHRR, cylinder pressure and needle lift profiles over injection pressures from 200 to 1300 bar. As observed in the injection timing sweep, a consistent LTHR peak for diesel is observed at 340 CAD at all injection pressures. As the injection pressure is increased from 200 bar to 1300 bar, the AHRR schedule changes from showing distinct premixed and mixing controlled burn phases to predominantly premixed type combustion. Additionally, an interesting trend is observed in the ignition delay times in Fig. 12 – ignition delay times increase with increasing injection pressure from 33 CAD at 200 bar injection pressure to about 40 CAD at 1300 bar injection pressure.

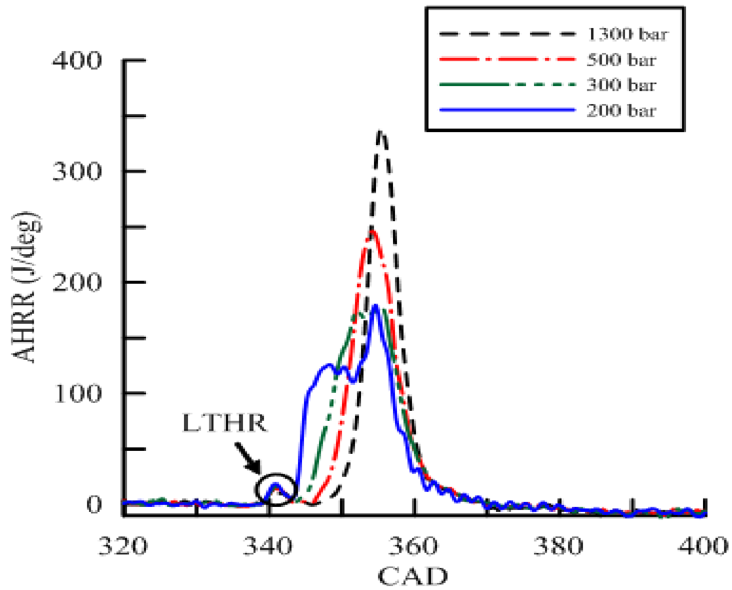

Figure 3.8 AHRR schedules at various injection pressures at 5.2 bar IMEP, 80 PES, N= 1500 RPM, Pin = 1.5 bar

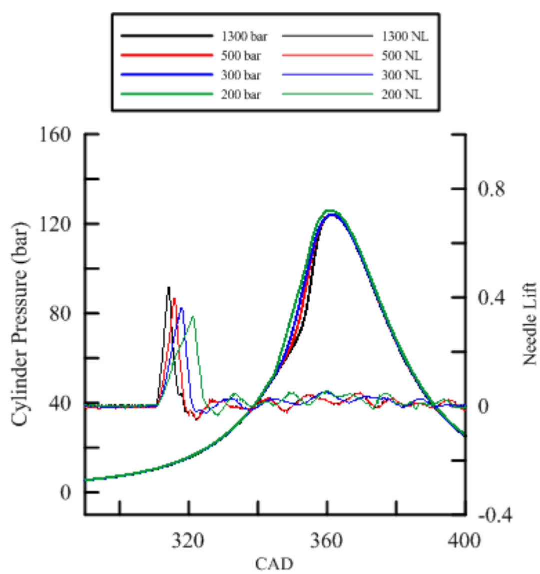

Figure 3.9 Cylinder pressure schedules at various injection pressures at 5.2 bar IMEP, 80 PES, N= 1500 RPM, Pin = 1.5 bar

As explained above, in this set of experiments, the injection timing was fixed at 50 DBTDC, the intake charge pressure was fixed at 1.5 bar, the only variable that is allowed to change is the injection pressure. So, to explain the counterintuitive ignition delay trends and the nature of combustion at these different injection pressures, it is instructive to examine the nature of the diesel spray at different injection pressures. Siebers [Siebers 1999] observes that the liquid length is invariant with injection pressures. This means that all else remaining a constant (as in this series of experiments), the vaporization rates (of the diesel fuel) are strongly governed by entrainment-induced mixing. The entrainment rate into the jet (of the surrounding gasoline-air mixture in this case) is proportional to the fuel jet exit velocity, the nozzle orifice diameter, the axial distance from the injector tip and densities of the fuel and air [Siebers 1999]. In the present case, the nozzle diameter is fixed, and since the injection timing is fixed, the air and fuel densities are also fixed. Therefore, the only contributing factor that affects entrainment rate is the injection velocity, which is dependent on injection pressure through the Bernoulli equation. Clearly, a higher injection velocity entails a faster entrainment rate and better mixing due to increased jet-induced turbulence. As a result, at higher injection pressures e.g 1300 bar, the diesel fuel is much better mixed than at lower injection pressures, e.g. 200 bar. In addition to the jet-induced mixing, another important factor that influences the overall mixing and therefore the ignition delay is the duration between end of injection (EOI) and start of combustion (SOC or CA5). At 200 bar injection pressure, as indicated by the needle lift profile in Figure 10, the injection duration is about 15 CAD (1.67 ms), the EOI is about 325 CAD and the SOC is about 343 CAD and the difference is about 18 CAD (2ms). At 500 bar, the EOI is about 320

CAD and SOC is around 348 CAD, and the difference is 28 CAD (3.1ms). Finally, at 1300 bar, the EOI at this condition is around 319 CAD while the SOC is around 357 CAD with a difference of nearly 38 CAD (4.2 ms).

From the above discussion, it is clear that with increasing injection pressure, the injection and combustion events are increasingly separated. For instance, at 200 bar injection pressure, both the jet-induced entrainment and mixing rates are slower due to low injection velocities; additionally, the EOI-SOC duration is the smallest. This means the diesel is relatively more stratified in the surrounding gasoline-air mixture. As a result, the combustion exhibits a two stage heat release, which is similar to that exhibited by classical diesel combustion. As the injection pressure is increased to 500 bar, both the jet-induced mixing and entrainment rates are enhanced. In addition, there is greater separation between EOI and SOC. This leads to optimal mixing so that the diesel can attain a "premixed-enough" state [Kalghatgi 2010], as a result the overall burn rate is slow but the local burn rates are sufficiently high. This is reflected by a sinusoidal heat release rate profile and increased AHRR peak magnitude. Further increase in injection pressure to 1300 bar indicates that the AHRR peak magnitude is significantly increased and the phasing of the AHRR peak is almost at TDC. At this injection pressure, the diesel fuel exits the nozzle at relatively high velocities. This results in enhanced entrainment and turbulent mixing of the surrounding gasoline-air mixtures into the spray. Moreover, the EOI-SOC separation is highest. The increased entrainment along with the long residence times result in the diesel fuel mixing well in the surrounding gasoline-air mixture. Consequently, when the in-cylinder temperature and pressure are high enough to support ignition, the prepared fuel mixture instantaneously ignites resulting in very high AHRR and shorter combustion durations. This combustion is similar diesel-assisted gasoline HCCI combustion observed at 170 DBTDC injection timing.

3.3.2 Ignition Delay, Maximum Pressure Rise Rate and Rate of Combustion

Figures 3.10 and 3.11 show the CA5, CA50, CA10-90, MPRR and Ignition delay times over the range of injection pressures investigated. The CA50 is phased closer to TDC as the injection pressure is increased from 200 bar to 1300 bar. The CA10-90 or combustion duration decreases with increasing injection pressure. MPRR and ignition delay times are observed to increase with increasing injection pressure. These observations further corroborate the AHRR analysis above. The increased ignition delay times at 1300 bar lead to very rapid combustion, which is characterized by a very short combustion duration, about 6 CAD, and a high MPRR, about 11 bar/CAD and is phased closest to TDC. At 500 bar injection pressure, the MPRR is about 8 bar/CAD and the ignition delay is about 35 CAD. CA50 is slightly retarded away from TDC and CA10-90 is 9 CAD. At this condition, the jet velocities are lower than at 1300 bar, therefore, the entrainment rates are correspondingly lower. At 200 bar injection pressure, the MPRR is about 7 bar/CAD and the ignition delay is about 33 CAD. CA50 is most retarded away from TDC and CA10-90 is the longest at 13 CAD. At this condition, the jet velocities are the lowest among the injection pressures investigated; therefore, the entrainment rates are the lowest. The decreased entrainment and mixing rates and reduced residence times result in diesel retaining heterogeneity; as a result, the combustion duration is longer and also shows distinct two stage heat release.

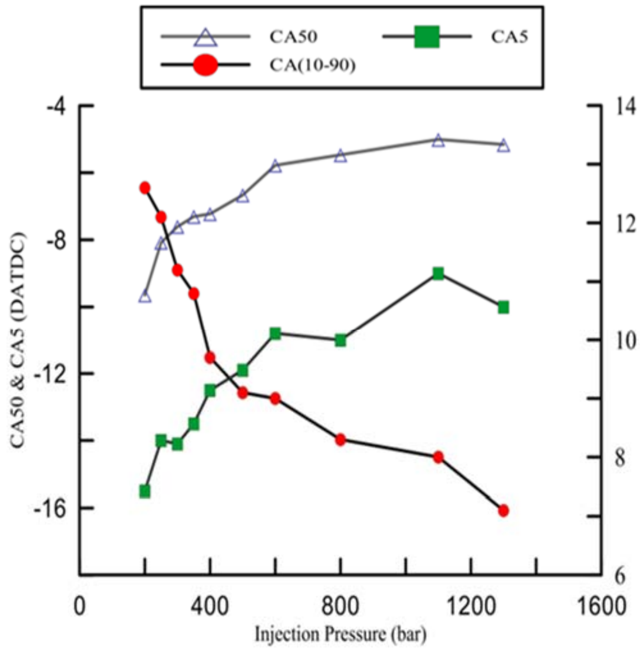

Figure 3.10 Figure 3.10 CA5, CA50 and CA10-90 at various injection pressures at 5.2 bar IMEP, 80 PES, N= 1500 RPM, Pin = 1.5 bar

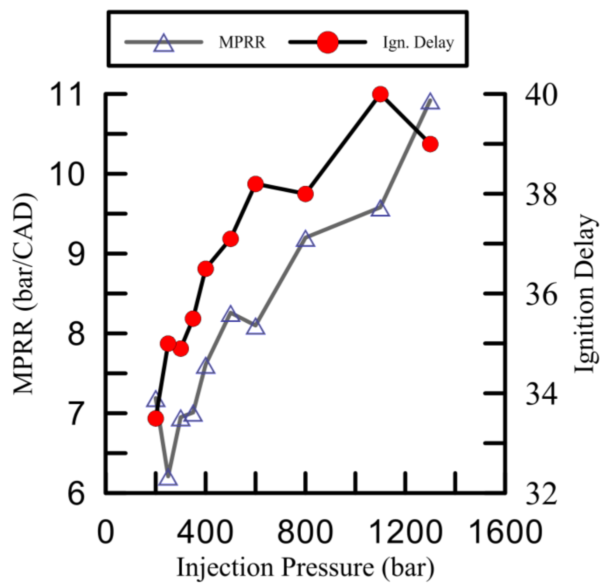

Figure 3.11 MPRR and Ignition delay at various injection pressures at 5.2 bar IMEP, 80 PES, N= 1500 RPM, Pin = 1.5 bar

3.3.3 Fuel Conversion Efficiency and Combustion Efficiency

Figure 3.12 shows the combustion efficiency and IFCE trends with injection pressures. Combustion efficiency remains unchanged; however, the indicated fuel conversion efficiency increases with increasing injection pressure from 39% at 200 bar to 43% at 1300 bar. As explained before, at 200 bar injection pressure, combustion is characterized by CA50 that is retarded from TDC and long CA10-90 duration. This indicates that the volume available for expansion is reduced; therefore, the net indicated work is also reduced. In contrast, combustion at 1300 bar is characterized by CA50 that is phased closer to TDC and short combustion duration; therefore, the indicated fuel conversion efficiencies are higher. It is interesting to note that the combustion efficiency is unaffected by injection pressure. This implies that engine-out HC emissions are also unaffected by changes in injection pressure, which is confirmed in Figure 3.14.

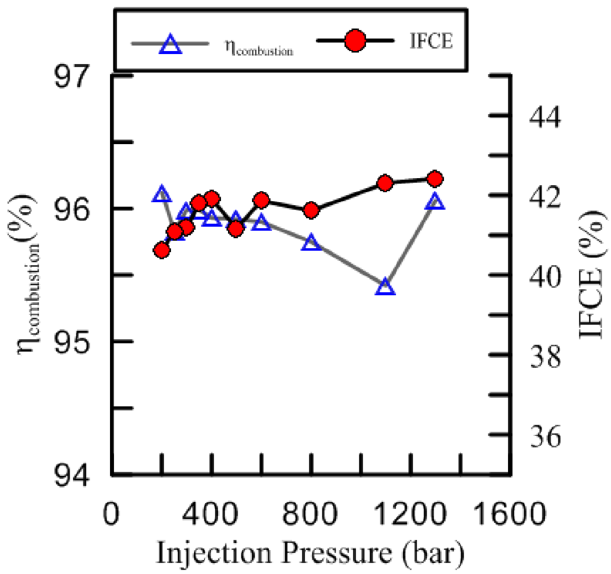

Figure 3.12 Combustion and Indicated Fuel Conversion efficiencies at various injection pressures at 5.2 bar IMEP, 80 PES, N= 1500 RPM, Pin = 1.5 bar, IFCE for baseline diesel were 45% (Rail pressure = 500 bar, Pin = 1.5 bar, injection timing = 10 DBTDC)

3.3.4 Emissions

Figures 3.13 shows ISNOx and smoke emissions trends with injection pressures. As injection pressure increases from 200 bar to 1300 bar, ISNOx emissions decrease drastically from 4.5 g/kWhr to near-zero levels (less than 0.1 g/kWhr) while the smoke emissions levels are constant (less than 0.1 FSN) and are essentially un-affected by injection pressure. The increased NOx at 200 bar may be attributed to two factors, (1) increased heterogeneity due to reduced mixing and entrainment rates due to low injection velocities and (2) the injection duration is longer to keep the same diesel injected quantity. As a result, the ensuing combustion occurs at high local temperatures that favor thermal NOx formation. In contrast, as injection pressure increases, the injection duration also decreases, and there is increased separation between the injection and combustion processes. As a result, the ignition delays are longer and combustion is increasingly homogeneous and occurs at low local temperatures thus avoiding thermal NO formation. The engine-out smoke emissions are low throughout due to the predominantly lean combustion process at all injection pressures.

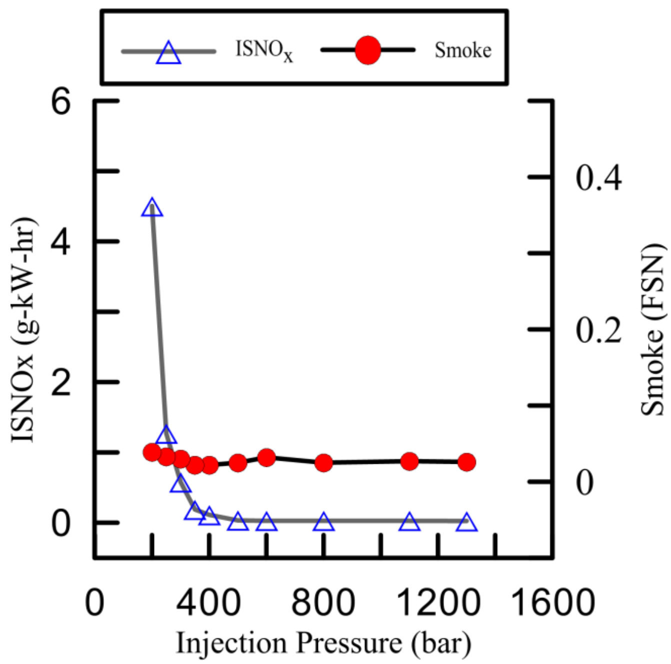

Figure 3.13 ISNOx and smoke at various injection pressures at 5.2 bar IMEP, 80 PES, N= 1500 RPM, Pin = 1.5 bar, ISNOx and smoke for baseline diesel were 9.63 g/kWhr and 0.37 FSN respectively (Rail pressure = 500 bar, Pin = 1.5 bar, injection timing = 10 DBTDC)

Figure 3.14 shows ISHC and ISCO emissions trends with injection pressures. The ISHC emissions are essentially unaltered with injection pressure. This is consistent with the fact that the combustion efficiencies are also un-changed with injection pressures. Also, bulk of the HC is likely from the crevices. Since the boost pressure is maintained a constant, the mass trapped in the crevices would remain unchanged with increasing injection pressure. Additionally, with increasing injection pressure, the CA50 is located closer to the TDC; therefore, bulk of the combustion process is complete near TDC. Since fuel oxidation rates are much faster than CO oxidation rates, the HC from the crevices would be oxidized to CO at these high bulk temperatures. The ISCO emissions decrease with increasing injection pressures. This is likely related to the degree of mixing achieved in the combustion chamber. For instance, at 1300 bar the nozzle exit velocities are higher and the resulting jet has considerable momentum to enhance surrounding gasoline-air entrainment rates and turbulent mixing. Moreover, the long residence times between the EOI and SOC allow for additional mixing. The resulting combustion is fast and is essentially complete before TDC where the bulk temperatures are high enough to promote $CO \rightarrow CO_2$ conversion, thereby reducing engine-out CO emissions.

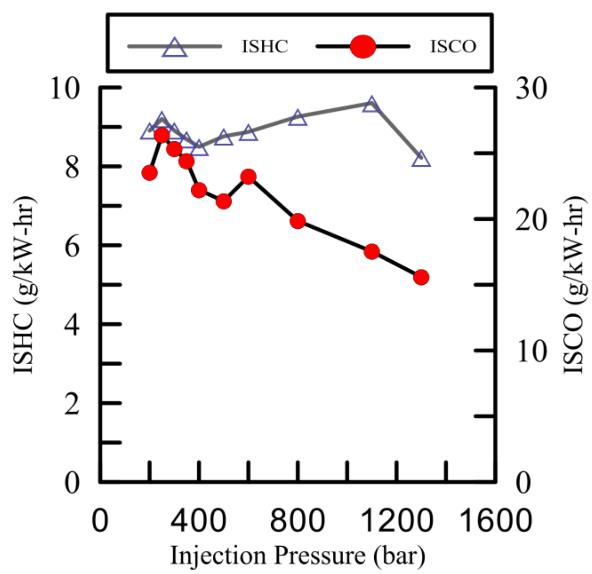

Figure 3.14 ISHC and ISCO at various injection pressures at 5.2 bar IMEP, 80 PES, N= 1500 RPM, Pin = 1.5 bar

The ISNOx, smoke, ISHC, and ISCO emissions trends with injection pressures are somewhat counterintuitive. Martin et al. [Martin 2008] and Cheng et al. [Cheng et al. 2010] have verified through optical diagnostic studies that early direct injection diesel LTC suffered from high NOx and smoke emissions due to pool fires and the level of HC and CO emissions were related to the intensity of the pool fires. Early injection of diesel fuel results in spray-wall and/or spray-piston impingement, which leads to pool fires just after the onset of combustion. These pool fires are characterized by diffusion flames that provide fuel-rich/stoichiometric combustion zones needed for both smoke and NOx formation. However, in the case of diesel-gasoline LTC, the NOx, smoke emissions (Fig. 3.13) are observed to decrease, and HC and CO emissions (Fig. 3.14) are either un-altered to slightly decrease with increasing injection pressures. This can be explained from the fact that the amount of diesel injected at the early injection timing of 50 DBTDC is small (contributing only 20% of total fuel energy input) so that even at high injection pressures where there are possible spray-wall and spray-piston interactions, the chances of an intense pool fire development is a remote possibility. Consequently, the development of conditions conducive for NOx and smoke emissions are avoided; however, the spray-wall interactions could render a significant amount of the injected diesel fuel unavailable to initiate combustion of the lean premixed gasoline-air mixture. This results in slower overall combustion rates and low bulk temperatures, which leads to partial fuel oxidation and high HC and CO emissions.

3.4 Boost Pressure: Performance and Emissions

The engine was operated at 5.2 bar IMEP, 1500 rev/min and 80 PES at 50 DBTDC SOI and constant injection pressure of 500 bar while boost pressure was varied from 1.1 bar to 1.8 bar.

3.4.1 Apparent Heat Release Rate and Cylinder Pressure

Figures 3.15 and 3.16 show the cylinder pressure and AHRR profiles for boost pressures from 1.1 to 1.8 bar at 5.2 bar IMEP, 1500 rev/min, 80 PES, 50 DBTDC SOI, and a constant injection pressure of 500 bar.. As boost pressure is increased, the cylinder pressures during compression as well as the peak cylinder pressures are higher. However, the rate of pressure rise is steeper for the lower boost pressures. This is reflected in the AHRR profiles, which show a more delayed onset of combustion followed by very rapid heat release rates and increasingly high peak AHRR as boost pressure is decreased. A consistent LTHR peak is also observed at 340 CAD at all boost pressures. As boost pressure is increased or decreased from 1.4 bar, the AHRR profile changes shape from the smooth sinusoidal profile. For instance, at Pin = 1.1 bar, the AHRR is very rapid and combustion duration is reduced substantially. On the other hand, as Pin is increased to 1.8 bar, the SOC is advanced and the peak AHRR is reduced. These trends clearly demonstrate the significant impact of Pin on the overall combustion process.

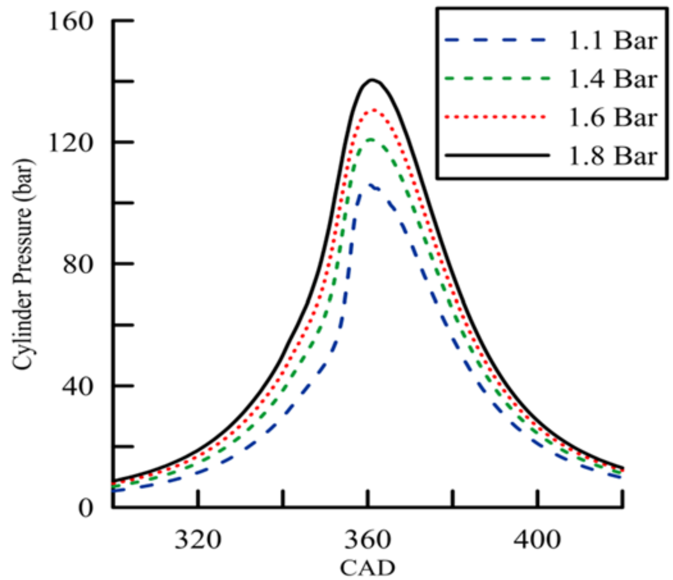

Figure 3.15 Cylinder pressure schedules at various boost pressures, 5.2 bar IMEP, 80 PES, N= 1500 RPM, Pinj = 500 bar

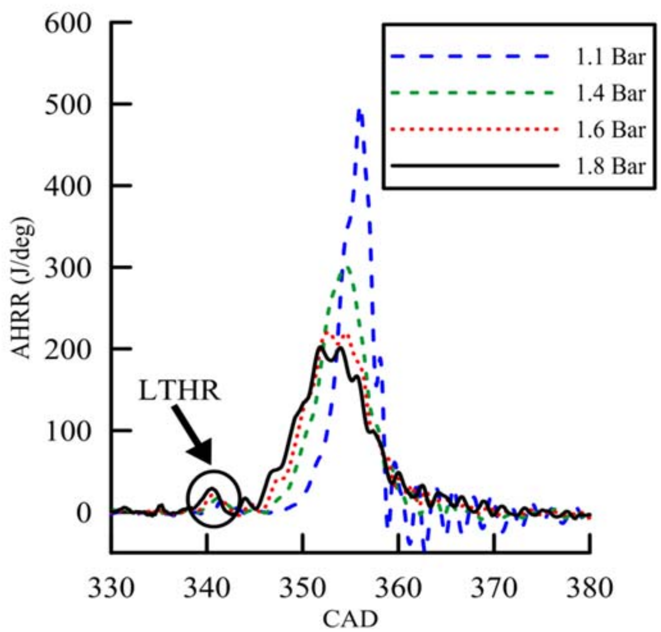

Figure 3.16 AHRR schedules at various boost pressures, 5.2 bar IMEP, 80 PES, N= 1500 RPM, Pinj = 500 bar

3.4.2 MPRR, Overall Equivalence ratio (ϕ), Ignition Delay and Combustion Rate

Figure 3.17 shows variations of MPRR, overall equivalence ratio (ϕ), ignition delay with boost pressure and Fig. 3.18 shows trends for CA5, CA50, and CA10-90 for different boost pressures. As boost pressure is decreased from 1.8 bar to 1.1 bar, ϕ increases (as expected) from 0.2 to 0.34, the MPRR increases from 8 bar/CAD to nearly 14 bar/CAD, and the ignition delay increases from 29 CAD to 40 CAD. As boost is decreased, in-cylinder pressures during compression decrease, thus increasing the ignition delay period. On the other hand, since ϕ also increases as boost is decreased, the combustion rates are more rapid as evident from Fig. 3.16, and therefore, MPRR also increases. Clearly, at least from the perspective of limiting MPRR to reasonably low values, it is beneficial to utilize relatively high boost pressures. For all of these cases, the COV of IMEP was fairly low, i.e., between 1.2 – 2%.

3.4.3 Fuel Conversion Efficiency, Combustion Efficiency and Emissions

The influence of boost pressure on IFCE, combustion efficiency, ISNOx, smoke, ISHC, and ISCO emissions are presented in Figs. 3.19-3.21. As boost pressure is decreased, the IFCE increases slightly from 41% at 1.8 bar to 43% at 1.3 bar before decreasing to 41.6% at 1.1 bar. This trend is likely the combined outcome of the CA5, CA50, and CA10-90 trends shown in Fig. 19. While CA5 and CA50 are retarded with decreasing boost pressure, CA10-90 is also decreased, thus leading to slightly higher IFCEs. The combustion efficiency is also increased slightly as boost pressure is reduced. This is a direct consequence of the sharp decrease in ISCO emissions as boost pressure is decreased, likely due to the more rapid AHRR and higher ϕ values. On the other hand, as seen from Figure 3.20, the faster heat release rates and presumably higher local temperatures at lower boost pressures lead to a sharp increase in ISNOx emissions for boost pressures lower than 1.5 bar. However, the ISHC and smoke emissions remain nearly invariant with boost pressure while ISCO emissions increase with increasing boost pressure.

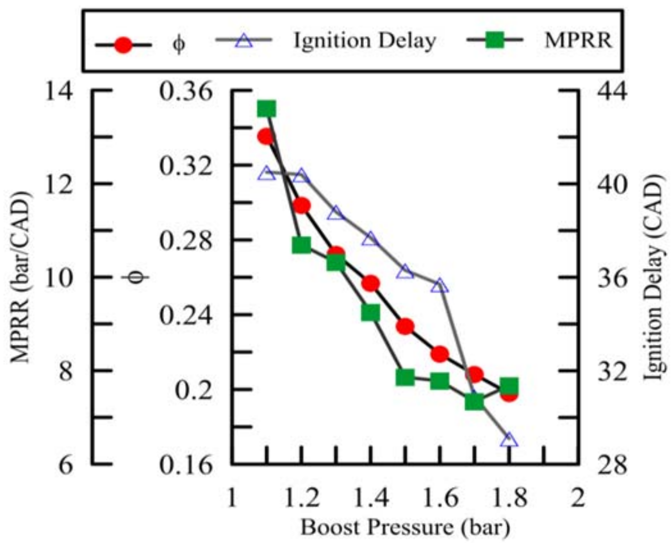

Figure 3.17 MPRR, overall equivalence ratio (ϕ), and ignition delay at various boost pressures, 5.2 bar IMEP, 80 PES, N= 1500 RPM, Pinj = 500 bar

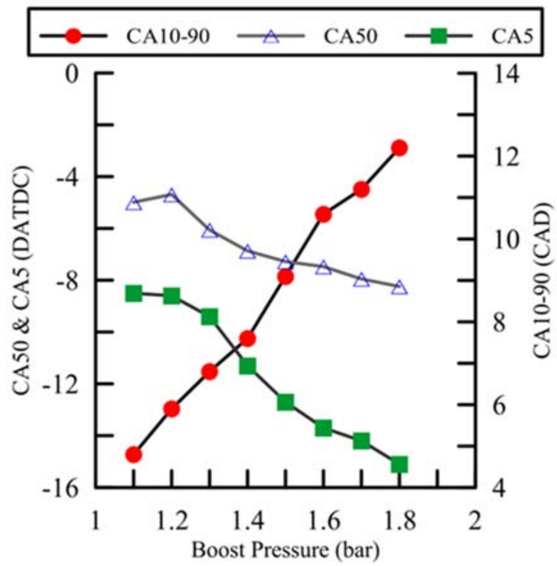

Figure 3.18 CA5, CA50, and CA10-90 at various boost pressures, 5.2 bar IMEP, 80 PES, N= 1500 RPM, Pinj = 500 bar

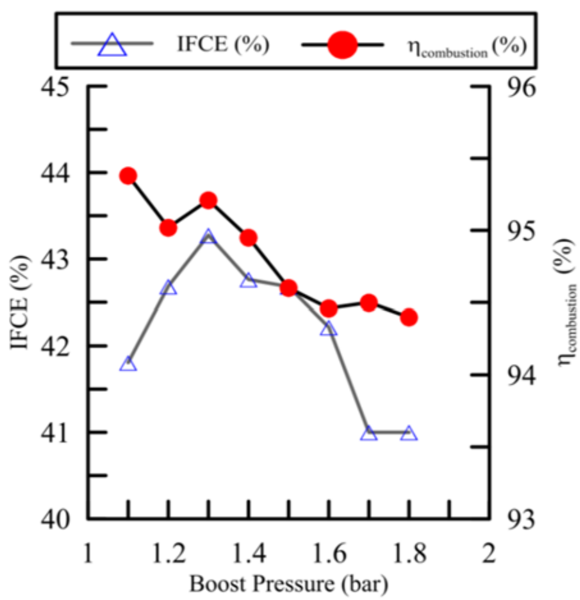

Figure 3.19 Combustion and Indicated Fuel Conversion efficiencies

Combustion and Indicated Fuel Conversion efficiencies at various boost pressures, 5.2 bar IMEP, 80 PES, N= 1500 RPM, Pinj = 500 bar, IFCE for baseline diesel were 45% (Rail pressure = 500 bar, Pin = 1.5 bar, injection timing = 10 DBTDC)

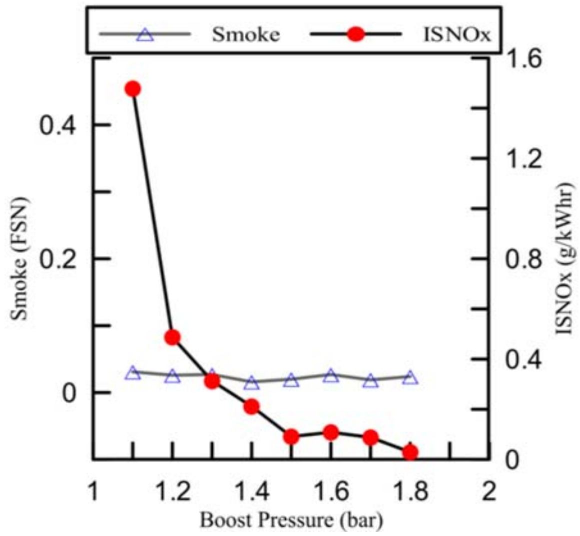

Figure 3.20 ISNOx and Smoke

ISNOx and Smoke at various boost pressures, 5.2 bar IMEP, 80 PES, N= 1500 RPM, Pinj = 500 bar, ISNOx and smoke for baseline diesel were 9.63 g/kWhr and 0.37 FSN respectively (Rail pressure = 500 bar, Pin = 1.5 bar, injection timing = 10 DBTDC)

The ISCO and ISHC trends are interesting and warrant closer scrutiny. With increasing boost pressures, the mass trapped within the crevices would also be high. However, since the since combustion is essentially complete at TDC at all boost pressures, the unburned crevice HC are likely oxidized. As a result, the net engine-out HC emissions remain unchanged; but, the ISCO emissions increase drastically with increasing boost pressures. It is apparent that the primary product of fuel oxidation is CO, and therefore there is a significant amount of CO from the combustion process. However, the oxidation of CO → CO_2 occurs much later in the overall reaction process; typically CO oxidation does not start until all of the fuel and intermediate hydrocarbons are consumed (this is because hydrocarbon oxidation is much faster than CO oxidation) [Glassman 1996]. Once the hydrocarbon fragments are consumed, the OH radical concentration increases to high levels and this aids the oxidation of CO via the following reaction:

$$CO + OH \rightarrow CO_2 + H \tag{7}$$

But, the rate of the above reaction does not increase appreciably until about 1100 K or higher temperatures. In the present case, since bulk of the combustion is complete around TDC, the initial high temperatures near TDC during expansion support fuel (or HC) oxidation. For instance, the peak bulk temperatures (not shown here) are of the order of 1550 K at 1.1 bar compared to 1300 K at 1.8 bar. Also, the bulk cylinder temperatures decrease rapidly with expanding cylinder volume. Therefore, the $CO \rightarrow CO_2$ conversion is impeded with increasing boost pressures since the peak bulk temperatures were lower to start with, as a consequence the CO chemistry freezes, thereby manifesting as higher engine-out CO emissions at higher intake boost pressures.

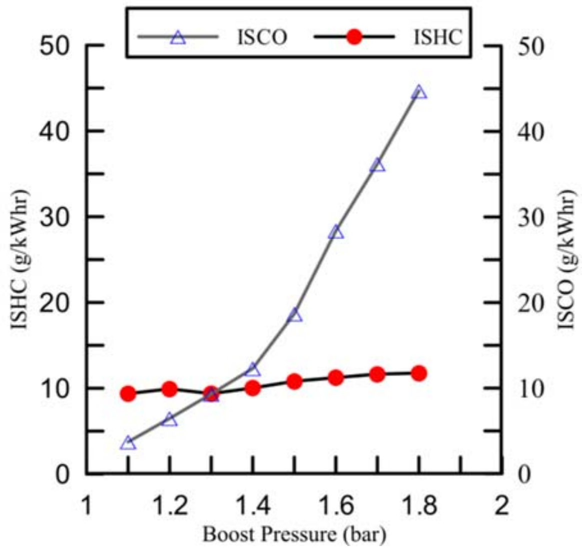

Figure 3.21 ISCO and ISHC emissions at various boost pressures, 5.2 bar IMEP, 80 PES, N= 1500 RPM, Pinj = 500 bar

CHAPTER IV

DIESEL-METHANE DUAL FUELING

4.1 Introduction

Diesel-ignited methane dual fuel combustion experiments were performed in a single-cylinder research engine (SCRE), outfitted with a common-rail diesel injection system and a stand-alone diesel injection driver. Methane was fumigated into the intake manifold using a needle valve. The engine was operated at a constant speed of 1500 rev/min, a constant load of 5.2 bar IMEP, and a constant methane energy substitution of 80%. Parameters such as diesel injection timing (SOI), diesel injection pressure, and boost pressure were varied to quantify their impact on engine performance and engine-out ISNOx, ISHC, ISCO, and smoke emissions. Advancing SOI from 30 DBTDC to 50 DBTDC reduced ISNOx from 14 g/kW-hr to near zero levels (0.015 g/kWhr); further advancement of SOI did not yield significant ISNOx reduction. Smoke emissions were less than 0.1 FSN at all SOIs, while ISHC ranged from 33 g/kWhr at 60DBTDC to 84 g/kWhr at 10 DBTDC. ISCO had the lowest value of 12.3 g/kWhr at 50 DBTDC but it increased on either advancing or retarding from that point. Indicated fuel conversion efficiencies were ~ 28-35%. An injection pressure sweep from 200 to 1300 bar at 60 DBTDC SOI showed that very low injection pressures lead to more heterogeneous combustion and higher ISNOx and ISHC emissions, whereas ISCO followed the opposite trend of increasing with increase in injection pressure. Smoke remained unaffected. A boost pressure sweep from 1.1 to 1.8 bar at 60 DBTDC SOI showed very rapid combustion for the lowest boost conditions, leading to higher ISNOx emissions, lower ISCO and ISHC emissions, while smoke remained unaffected by boost pressure variations. The pressure rise rates decreased with lower boost cases and the combustion efficiency increased.

4.2 Pilot Injection Timing: Performance and Emissions

The engine was operated at 5.2 bar IMEP, 1500 rev/min and 80 PES while diesel pilot injection timing was varied from 10 DBTDC to 110 DBTDC. The diesel injection pressure was maintained constant at 500 bar. The intake manifold pressure was set at 1.5 bar and no EGR was used.

4.2.1 Apparent Heat Release Rate and Cylinder Pressure

Figures 4.1 and 4.2 show the AHRR and cylinder pressure profiles at different injection timings. As the injection timing is advanced from 10 to 110 DBTDC, the shape of the AHRR changes significantly. At 30 DBTDC, fuel injection begins at 330 CAD and ends at 340 CAD. There are two distinct peaks and no significant low temperature heat release (LTHR) peak. Combustion is observed to start around 341 CAD, which shows separation between end of injection (EOI) and start of combustion (SOC) is very small, about 1 CAD. This also indicates that the diesel is injected at high enough cylinder temperatures; as a result, there are no significant low temperature reactions that would warrant LTHR. At 40 DBTDC, fuel injection begins at 320 CAD and ends at around 330 CAD. The main combustion event starts around 337 CAD, which is roughly 7 CAD after EOI which gives the diesel a lot more residence time to mix with methane air mixture and a distinct LTHR peak is observed at around 339 CAD, which is likely due to low temperature reactions leading to heat release from the high cetane diesel fuel. Unlike the diesel gasoline case, we do not see two distinct peaks for the 30 DBTDC and 40 DBTDC cases here. As the injection timing is advanced to 50 DBTDC, the LTHR is still prominent since the separation between EOI (320 CAD) and SOC (335 CAD) is around 15 CAD. Clearly, the injection and combustion events are beginning to get increasingly separated.

Table 4.1 Measured and emissions calculated equivalence ratios for various injection timings

Injection Timing (ºBTDC)	Φ (measured)	Φ(emissions)
10	0.389	0.348
20	0.342	0.32
30	0.328	0.3
40	0.315	0.29
50	0.303	0.274
60	0.296	0.273
70	0.303	0.282
80	0.309	0.285
90	0.325	0.294896
100	0.332	0.30153
110	0.344	0.308577

As SOI is advanced further from 50 DBTDC to 110 DBTDC, the magnitude of heat release decreases and the peak heat release is phased almost at and beyond TDC. As we keep advancing from 50 DBTDC to 110 DBTDC, the LTHR vanishes and a "well mixed" combustion of diesel-methane is observed. The AHRR peak first advances from 10 to 30 DBTDC and then is retarded with advanced SOIs.

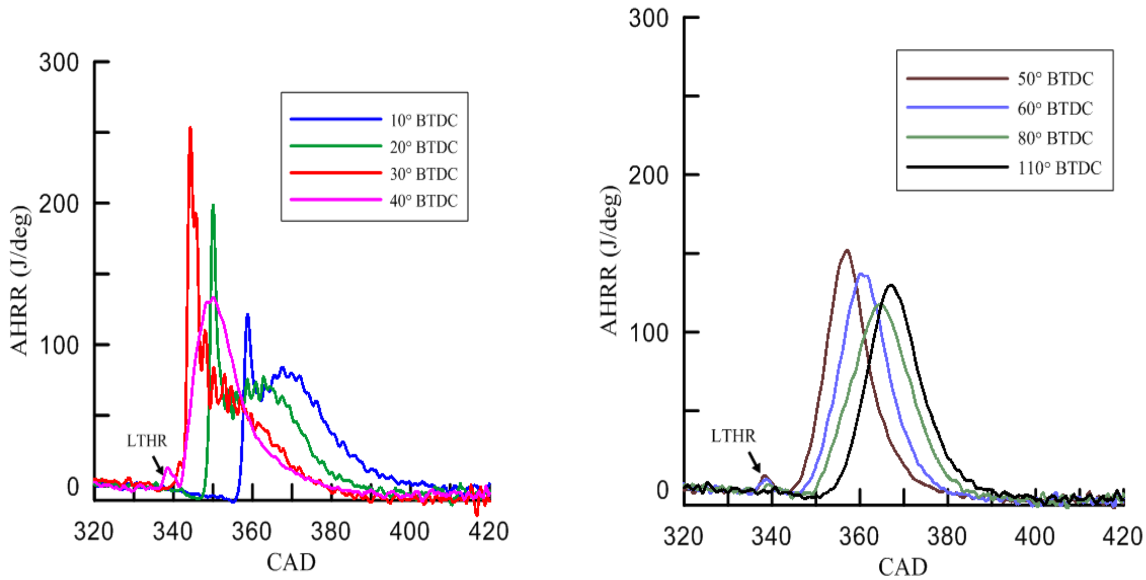

Figure 4.1 AHRR schedules at various injection timings at 5,2 bar IMEP, 80 PES, N=1500RPM, Pin= 1.5 bar

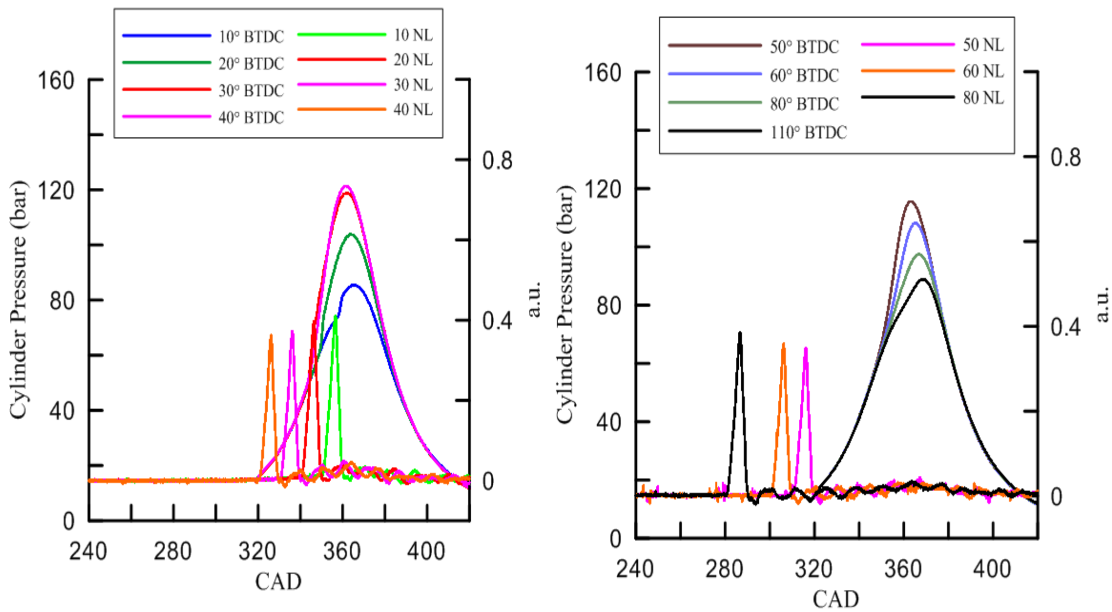

Figure 4.2 Cylinder pressure and needle lift schedules at various injection timings at 5,2 bar IMEP, 80 PES, N=1500RPM, Pin= 1.5 bar

4.2.2 Ignition Delay, Maximum Pressure Rise Rate, Combustion Phasing and CA 10-90 duration

Figures 4.3 and 4.4 show ignition delay, MPRR, CA5, CA50 and CA10-90 trends over the range of SOIs from 10-110 DBTDC at 80 PES methane. Ignition delay increases with increasing injection advance from about 9.7 CAD at 10 DBTDC to 110.2 CAD at 110 DBTDC. This increase in ignition delay is what causes longer residence times thereby providing for better mixing of diesel and methane –air mixture. CA50 is seen to shift from ATDC to BTDC while advancing injection timing from 10 to 40DBTDC, but then as we keep on advancing the CA50 shifts back to ATDC. This may be because of the heterogeneous combustion taking place in the 20-40 DBTDC range. It is also verified by high MPRR on advancing from 10-30 DBTDC, followed by the decrease between 10-110 DBTDC. Also from Figure 4.4, the CA10-90 (combustion durations) for 20-40

DBTDC decreases from 22 CAD (2.44ms) to 15.9 CAD (1.76ms), and between 50-110 DBTDC, combustion durations increase only slightly.

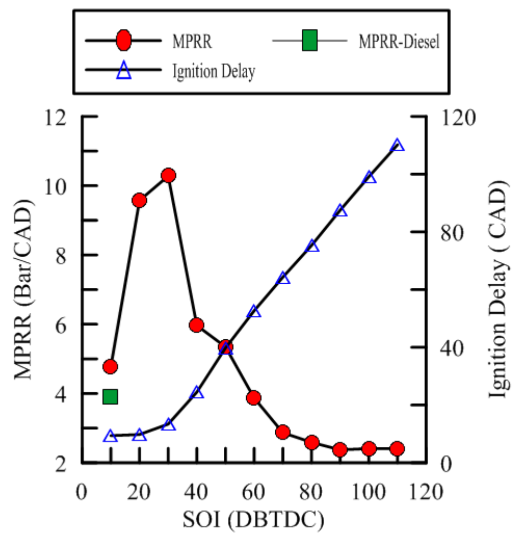

Figure 4.3 MPRR and Ignition delay at various injection timings at 5.2 bar IMEP, 80 PES, N= 1500 RPM, Pin = 1.5 bar

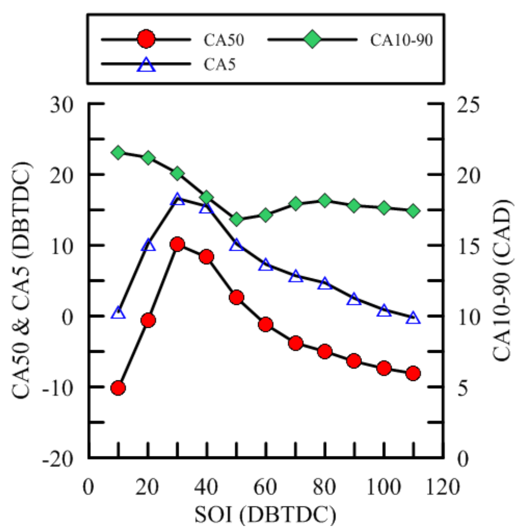

Figure 4.4 CA5, CA50 and CA10-90 at various injection timings at 5.2 bar IMEP, 80 PES, N= 1500 RPM, Pin = 1.5 bar

4.2.3 Fuel Conversion Efficiency and Combustion Efficiency

Figure 4.5 shows the indicated fuel conversion and combustion efficiencies between 10 and 110 DBTDC SOI at a constant load of 5.2 bar IMEP and 80 PES. Clearly, the combustion efficiency increases with increasing injection advance from 20 to 70 DBTDC, indicating that the HC and CO emissions are low at these injection timings. This is confirmed in Figure 4.6. Also, the IFCE increases from 28% at 10 DBTDC to 35% at 70 DBTDC. This increase in IFCE can be attributed to the increased combustion efficiencies at the advanced injection timings. Note that as we keep advancing further from 80 DBTDC to 110 DBTDC, both the combustion efficiency and the IFCE start to decrease.

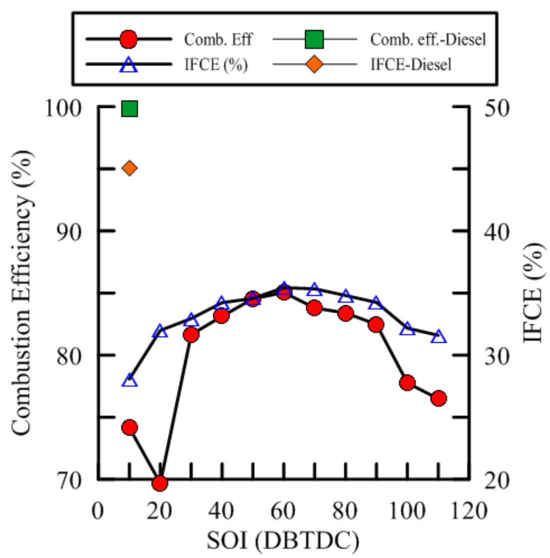

Figure 4.5 Combustion and Indicated Fuel Conversion efficiencies at various injection timings at 5.2 bar IMEP, 80 PES, N= 1500 RPM, Pin = 1.5 bar

4.2.4 Emissions

Figure 4.6 shows the ISCO and ISHC emissions trends between 10 and 110 DBTDC SOI at a constant load of 5.2 bar IMEP and 80 PES. ISCO decreases from about 26.53 g/kWhr at 10 DBTDC to 12.3 g/kWhr at 50 DBTDC and then increases to 44.63 g/kWhr at 110 DBTDC. ISHC decreases from 84.05 g/kWhr at 10 DBTDC to about 33.48 g/kWhr at 60 DBTDC and then increases to nearly 60.7 g/kWhr at 110 DBTDC.

For retarded injection timings of 10 DBTDC and 20 DBTDC the SOC occurs a lot closer to TDC, thereby giving very less time for the combustion process to occur. This is the reason for very high ISHC values at 10 DBTDC and 20 DBTDC. As we advance the injection timing from 20 to 40 DBTDC, the SOC occurs at nearly 340 CAD. Also a small LTHR peak is visible for the SOI of 40 DBTDC. This LTHR peak remains till about 80 DBTDC SOI and then vanishes. At retarded injection timings of 10-20 DBTDC and very advanced timings of 100-110 DBTDC, the CA50 occurs at nearly 10ºATDC and since the equivalence ratio is lean, high temperatures are not sustained due to rapid piston expansion, as a result the in-cylinder conditions are not conducive to support HC and CO oxidation; therefore both the ISHC and ISCO are high at those points. Also at very advanced injection timing of 100-110 DBTDC, the diesel is fairly well-mixed in the methane-air mixture. As a result, even if the temperature increases during the compression process it is not sufficient to foster HC and CO oxidation due to very lean conditions, therefore HC and CO are high. Looking at ISCO plot we see that CO emission is fairly low for SOIs between 40-60 DBTDC. This is because the CA50 is phased closer to TDC, so the bulk temperatures are higher and support CO oxidation in the expansion process. On further advancing from 60 to 80 DBTDC, there is a competition between HC and CO oxidation. Since HC oxidation rates are much faster than CO, HC is oxidized while CO freezes during expansion, thus increasing the CO emissions.

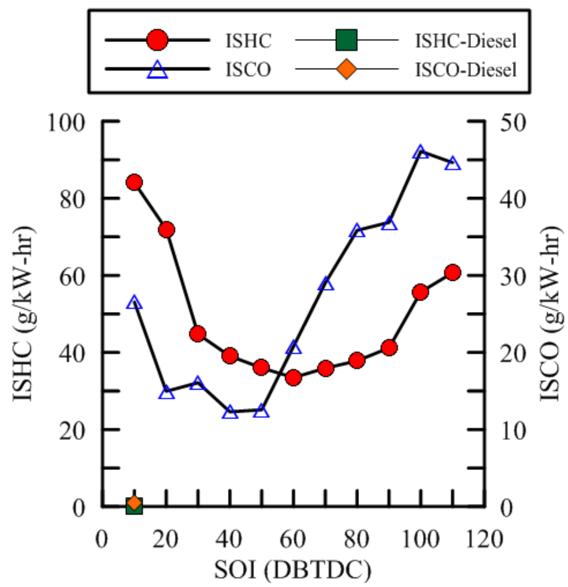

Figure 4.6 ISHC and ISCO emissions at various injection timings at 5.2 bar IMEP, 80 PES, N= 1500 RPM, Pin = 1.5 bar

The ISNOx and smoke emissions in Figure 4.7 show an interesting trend. On advancing the injection timing from 10 DBTDC to 30 DBTDC, the NOx emissions drastically increase from about 3.87 g/kWhr to about 14 g/kWhr. However, on further advancing the injection timing the NOx values dramatically drop from 14 g/kWhr to near zero levels (0.015 g/kWhr) and remain that way till 110 DBTDC. The smoke emissions remain unchanged throughout the injection timing sweep at less than 0.04 FSN. This dramatic NOx reduction is related to the increased residence times available for the diesel pilot to mix with the surrounding methane-air mixtures. This increased mixing with earlier injection advance results in increasingly homogeneous in-cylinder mixtures, which in-turn results in low local temperatures, much below the thermal NOx formation threshold temperatures of 1900 K.

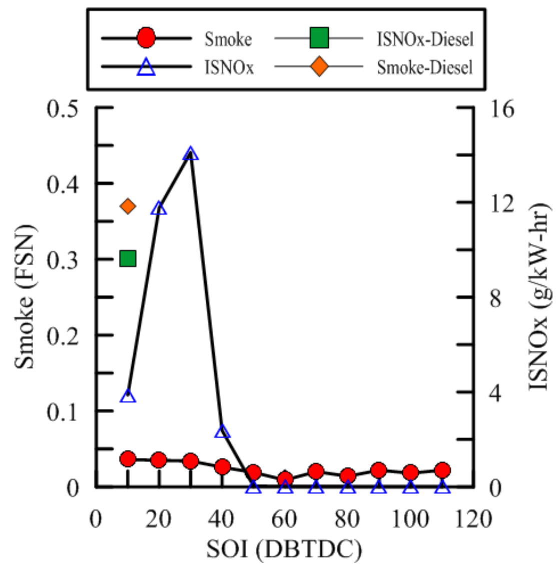

Figure 4.7 ISNOx and smoke emissions at various injection timings at 5.2 bar IMEP, 80 PES, N= 1500 RPM, Pin = 1.5 bar

Consequently, the NOx emissions are reduced to near-zero levels. The simultaneous reduction of NOx and smoke emissions is an indirect proof of the occurrence of low temperature combustion (LTC) under these conditions.

4.3 Rail Pressure: Performance and Emissions

The engine was operated at 5.2 bar IMEP, 1500 rev/min and 80 PES at 60 DBTDC SOI and constant boost pressure of 1.5 bar while injection pressure was varied from 200 bar to 1300 bar.

4.3.1 Apparent Heat Release Rate and Cylinder Pressure

Figure 4.8 and 4.9 show the AHRR and cylinder pressure over injection pressures from 200 to 1300 bar. Looking at the needle lift profile in Figure 4.9 we can say that the injection duration for 200 bar injection pressure is about 17 CAD (1.88 ms). The duration between EOI (317 CAD) and SOC (335 CAD) is about 18 CAD (2 ms). As observed in the injection timing sweep, a consistent LTHR peak for diesel is observed at roughly 338 CAD at all injection pressures. This is because the SOI is maintained at 60 DBTDC. As the injection pressure is increased from 200 bar to 1300 bar, the SOC is retarded. Also the magnitude of heat release increases with increase in injection pressure.

Table 4.2 Measured and emissions calculated equivalence ratios for various injection pressures

Injection Pressure	Φ (measured)	Φ(emissions)
1300	0.251708	0.255781
1100	0.25016	0.25535
800	0.252739	0.255944
600	0.255133	0.260506
500	0.259634	0.261664
400	0.262681	0.266071
350	0.260029	0.266996
300	0.274234	0.27246
250	0.268709	0.275957
200	0.275468	0.278788

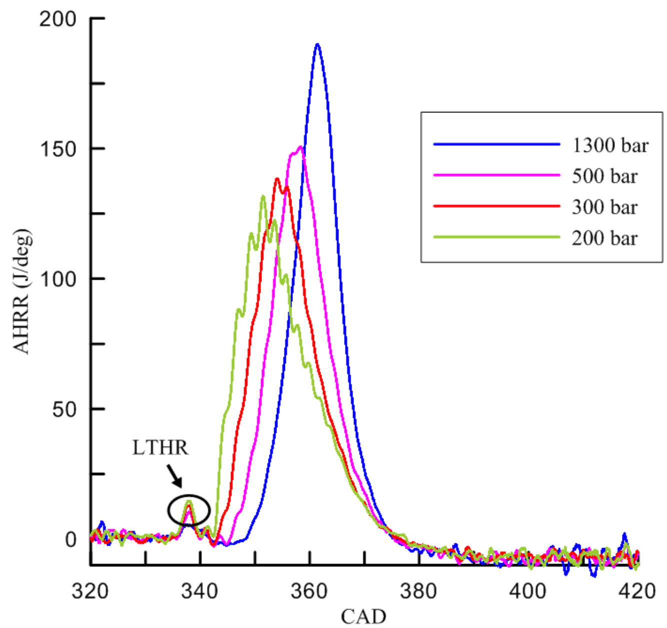

Figure 4.8 AHRR schedules at various injection pressures at 5,2 bar IMEP, 80 PES, N=1500RPM, Pin= 1.5 bar

From the AHRR plot Figure 4.8 it will be safe to assume that at and beyond 500 bar injection pressure the injected diesel has increased residence times to attain a "premixed-enough" state, as a result the overall burn rate is slow but the local burn rates are sufficiently high. This is reflected by the increased AHRR peak magnitude and retarded phasing of the AHRR curve. Further increase in injection pressure to 1300 bar indicates that the AHRR peak magnitude is significantly increased and the phasing of the AHRR peak is almost at TDC. At this injection pressure, the diesel fuel exits the nozzle at relatively high velocities. The increased jet momentum results in enhanced entrainment and turbulent mixing of the surrounding methane-air mixtures into the spray. The increased entrainment along with the long residence times result in the diesel fuel mixing well in the surrounding methane-air mixture. Consequently, when the in-cylinder temperature and pressure are high enough to support ignition, the prepared fuel mixture instantaneously ignites resulting in very high AHRR and shorter combustion durations.

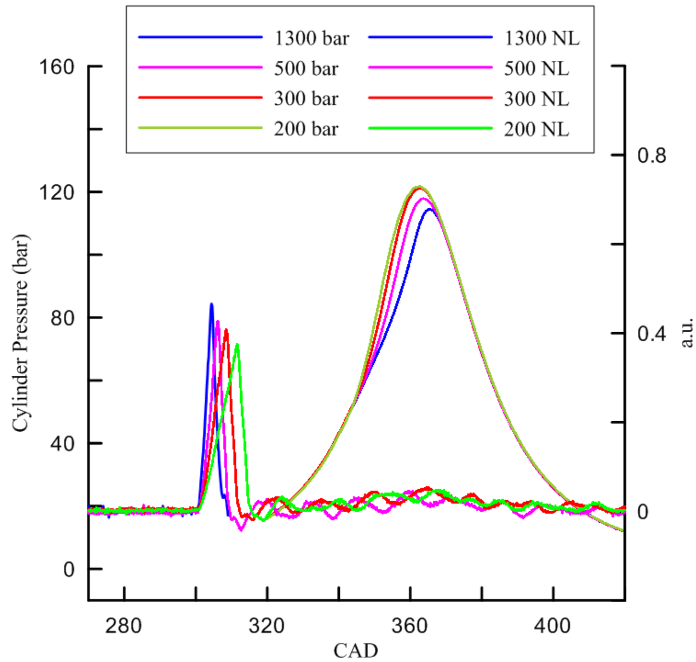

Figure 4.9 Cylinder pressure and needle lift schedules at various injection pressure at 5,2 bar IMEP, 80 PES, N=1500RPM, Pin= 1.5 bar

4.3.2 Ignition Delay, Maximum Pressure Rise Rate and Combustion Duration

Figures 4.10 and 4.11 show the CA5, CA50, CA10-90, MPRR and Ignition delay times over the range of injection pressures investigated. The CA50 is phased closer to TDC as the injection pressure is increased from 200 bar to 1300 bar. The CA10-90 or combustion duration decreases drastically with increasing injection pressure. Maximum pressure rise rate decreases and ignition delay times increase with increasing injection pressure. These observations further corroborate the AHRR analysis above. Increase in ignition delay for higher injection pressure leads to an increase in residence times for the diesel to mix with methane-air mixture, thereby creating a "well mixed" mixture at high injection pressures. However no significant change was observed in MPRR, and it remained in the range of 4-6 bar/CAD which was acceptable.

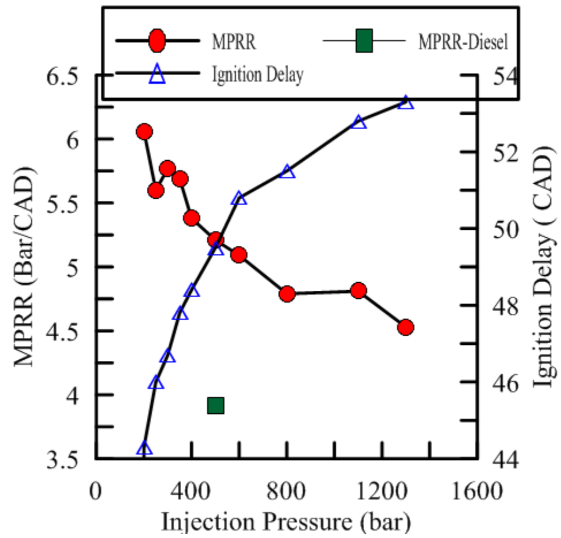

Figure 4.10 MPRR and Ignition delay at various injection pressures at 5.2 bar IMEP, 80 PES, N= 1500 RPM, Pin = 1.5 bar

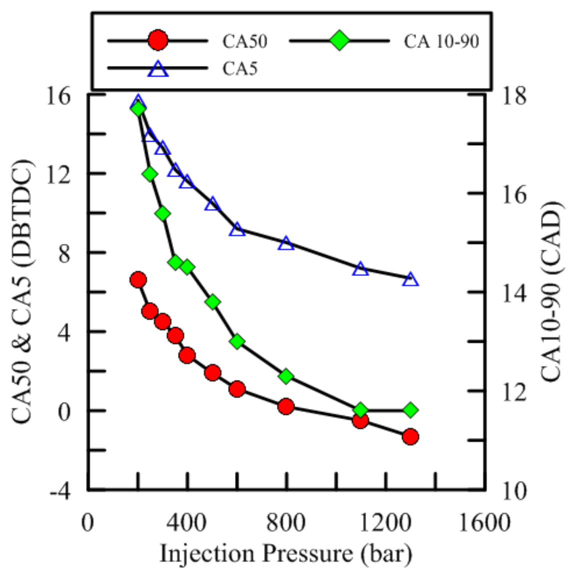

Figure 4.11 CA5, CA50 and CA10-90 at various injection pressures at 5.2 bar IMEP, 80 PES, N= 1500 RPM, Pin = 1.5 bar

4.3.3 Fuel Conversion Efficiency and Combustion Efficiency

Figure 4.12 shows the combustion efficiency and IFCE trends with injection pressures. A slight increase in combustion efficiency is observed as we increase the injection pressure from 200 to 1300 bar. Better combustion efficiency can be directly related to lower HC emissions, and that is clearly evident in Figure 4.13. The combustion at 1300 bar is characterized by CA50 that is phased closer to TDC and short combustion duration; therefore, the indicated fuel conversion efficiencies and combustion efficiencies are slightly higher.

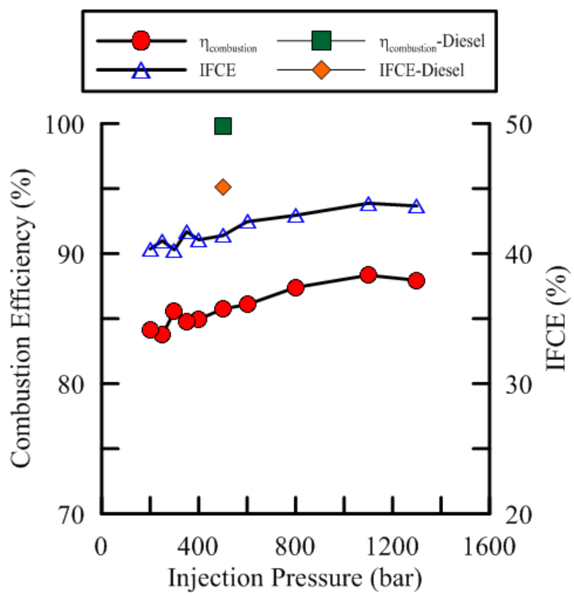

Figure 4.12 Combustion and Indicated Fuel Conversion efficiencies at various injection pressures at 5.2 bar IMEP, 80 PES, N= 1500 RPM, Pin = 1.5 bar

4.3.4 Emissions

Figure 4.13 shows ISNOx and smoke emissions trends with injection pressures. As injection pressure increases from 200 bar to 1300 bar, ISNOx emissions decrease drastically from 2.3 g/kWhr to near-zero levels (less than 0.1 g/kWhr) while the smoke emissions levels are constant (less than 0.1 FSN) and are essentially unaffected by injection pressure. The increased NOx at 200 bar is likely due to the fact that the injection duration is longer to keep the same diesel injected quantity. As a result, the combustion is more heterogeneous and is characterized by high local temperatures that favor thermal NO formation. In contrast, as injection pressure increases, the injection duration also decreases, and there is increased separation between the injection and combustion processes. As a result, the ignition delays are longer and combustion is increasingly homogeneous and occurs at low local temperatures thus avoiding thermal NO formation. The engine-out smoke emissions are low throughout due to the predominantly lean combustion process at all injection pressures.

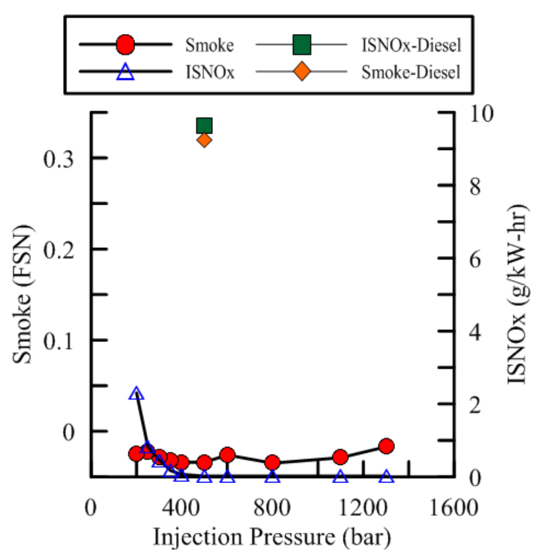

Figure 4.13 ISNOx and smoke emissions at various injection pressures at 5.2 bar IMEP, 80 PES, N= 1500 RPM, Pin = 1.5 bar

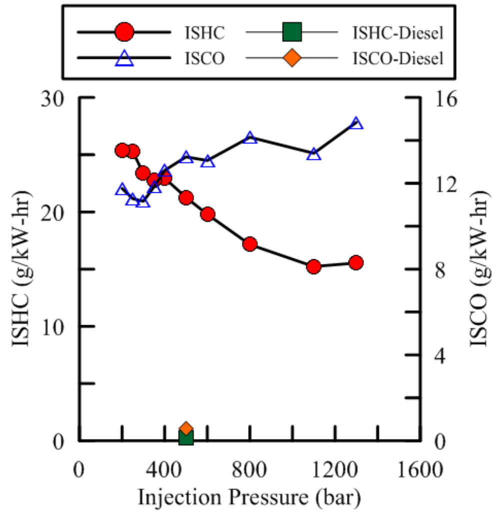

Figure 4.14 ISHC and ISCO emissions at various injection pressures at 5.2 bar IMEP, 80 PES, N= 1500 RPM, Pin = 1.5 bar

Figure 4.14 shows ISHC and ISCO emissions trends with injection pressures. The ISHC emissions change from 25 g/kW-hr to 15 g/kW-hr with increase in injection pressure. This is consistent with the fact that the combustion efficiencies increase with increased injection pressures. The ISCO emissions on the other hand increase ever so slightly with increasing injection pressures. This may be due to the fact that at high injection pressures the fuel gets thoroughly mixed with the methane-air charge and makes a lean mixture, reducing the bulk temperature and thereby reducing $CO \rightarrow CO_2$ conversion, and in turn increasing the CO emissions.

4.4 Boost Pressure: Performance and Emissions

The effect of boost pressure (intake air pressure) variations (from 1.1 bar to 1.8 bar in steps of 0.1 bar) were quantified at 5.2 bar IMEP, 1500 rev/min, 80 PES, 60 DBTDC SOI, and at a constant injection pressure of 500 bar.

4.4.1 Apparent Heat Release Rate and Cylinder Pressure

Figures 4.15 and 4.16 show the cylinder pressure and AHRR profiles for boost pressures from 1.1 to 1.8 bar at 5.2 bar IMEP, 1500 rev/min, 80 PES, 60 DBTDC SOI, and a constant injection pressure of 500 bar. As boost pressure is increased, the cylinder pressures during compression as well as the peak cylinder pressures are higher. The heat release decreases in magnitude on increasing intake air pressure. An LTHR peak is also observed at 338 CAD at all boost pressures. As boost pressure is increased, the AHRR profile changes shape from the smooth sinusoidal profile. The magnitude of AHRR decreases with increasing the intake air pressure but the difference is not that significant. Also the peak AHRR is advanced with increase in boost pressure, and so is the SOC.

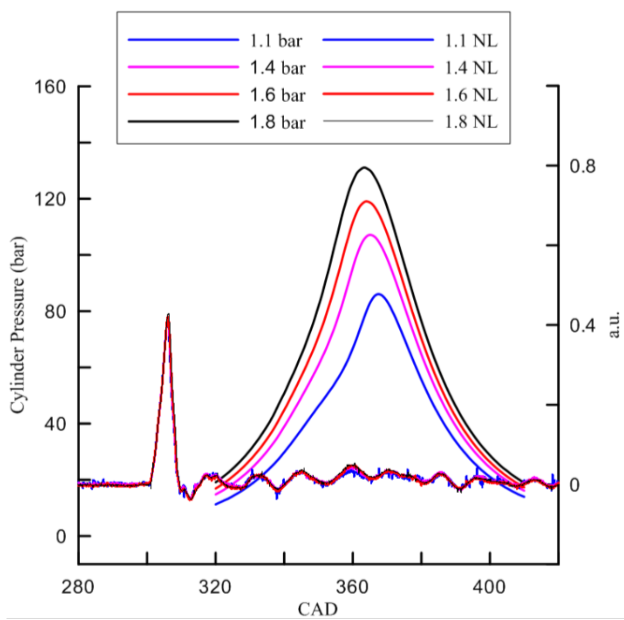

Figure 4.15 Cylinder pressure and needle lift schedules at various intake air pressures (Boost Pressures) at 5.2 bar IMEP, 80 PES, N=1500RPM, injection pressure= 500 bar

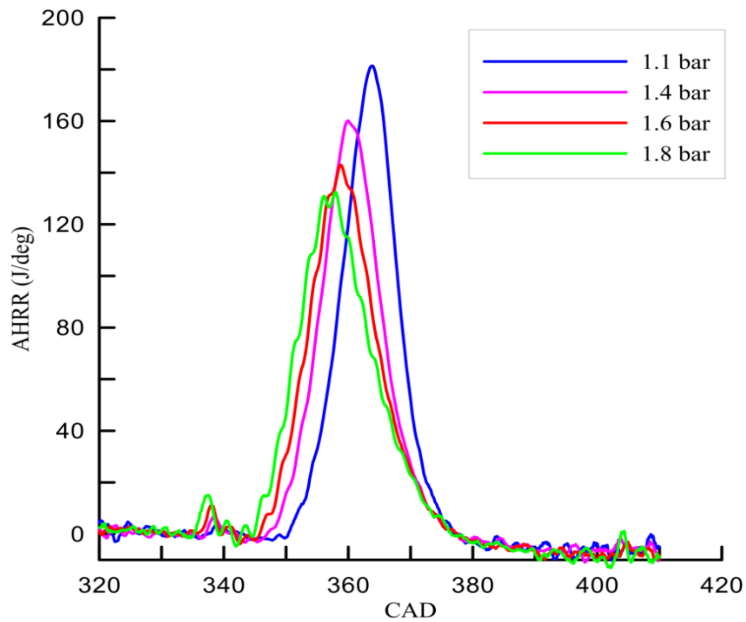

Figure 4.16 AHRR schedules at various boost pressures at 5.2 bar IMEP, 80 PES, N=1500RPM, injection pressure= 500 bar

4.4.2 MPRR, Overall Equivalence ratio (ϕ), Ignition Delay and Combustion Rate

Figure 4.17 shows variations of MPRR, overall equivalence ratio (ϕ), ignition delay with boost pressure and Fig. 4.18 shows trends for CA5, CA50, and CA10-90 for different boost pressures. As boost pressure is decreased from 1.8 bar to 1.1 bar, ϕ increases (as expected) from 0.21 to 0.35; however, the MPRR decreases from 5.23 bar/CAD to nearly 3.61 bar/CAD, and the ignition delay increases from 45 CAD to 52 CAD. Decrease in boost causes a decrease in in-cylinder pressures and temperatures, thus increasing the ignition delay period. On the other hand, since ϕ also increases as boost is decreased, the combustion rates are more rapid as evident from Fig. 4.16.

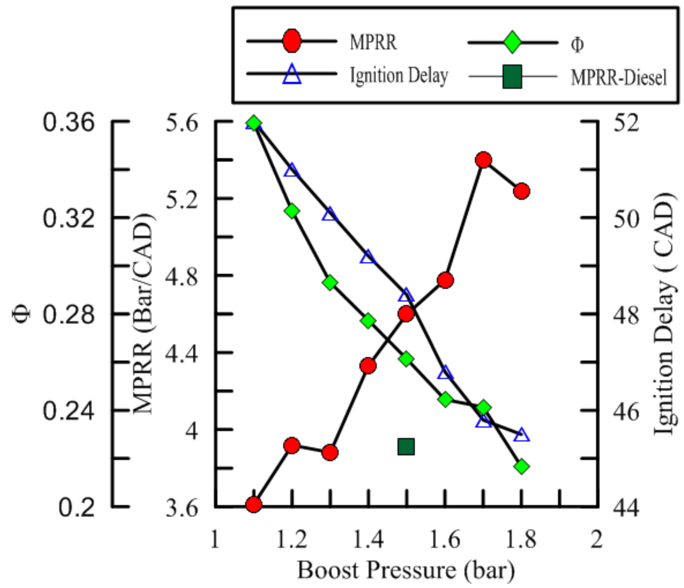

Figure 4.17 MPRR, Equivalence ratio (Φ) and Ignition delay at various injection pressures at 5.2 bar IMEP, 80 PES, N= 1500 RPM, injection pressure= 500 bar

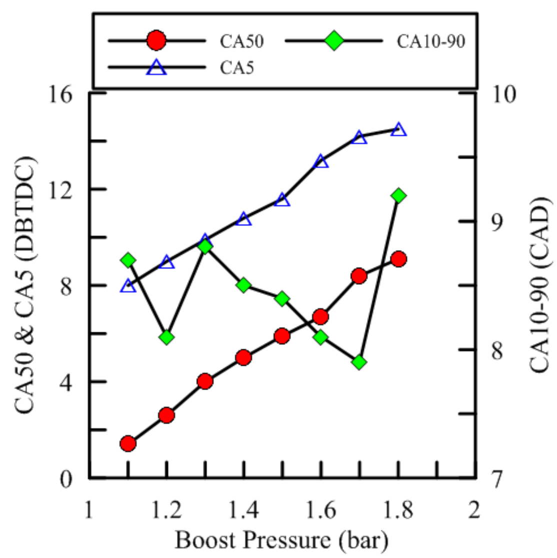

Figure 4.18 CA5, CA50 and CA10-90 at various boost pressures at 5.2 bar IMEP, 80 PES, N= 1500 RPM, injection pressure= 500 bar

4.4.3 Fuel Conversion Efficiency, Combustion Efficiency and Emissions

The influence of boost pressure on IFCE, combustion efficiency, ISNOx, smoke, ISHC, and ISCO emissions are presented in Figs. 4.19-4.21. As boost pressure is decreased, the IFCE increases slightly from 42% at 1.8 bar to 45% at 1.1 bar. The combustion efficiency is also increased slightly as boost pressure is reduced. This is again a direct consequence of the sharp decrease in ISCO and ISHC emissions as boost pressure is decreased, likely due to the more rapid AHRR and higher ϕ values. On the other hand, the faster heat release rates and presumably higher local temperatures at lower boost pressures lead to a sharp increase in ISNOx emissions for boost pressures lower than 1.3 bar. However, the smoke emissions remain nearly invariant with boost pressure.

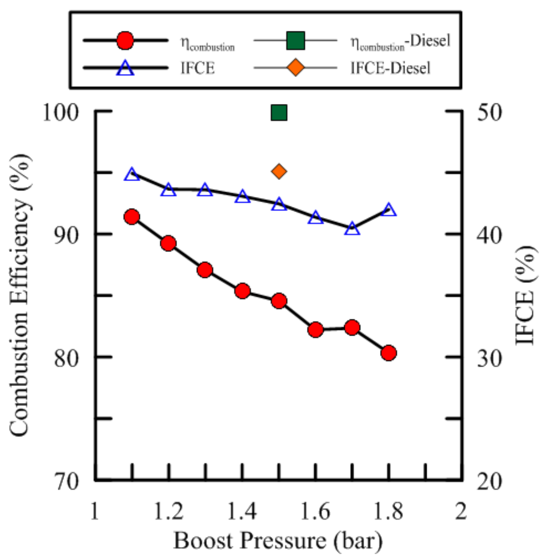

Figure 4.19 Combustion and Indicated Fuel Conversion efficiencies at various boost pressures at 5.2 bar IMEP, 80 PES, N= 1500 RPM, injection pressure= 500 bar

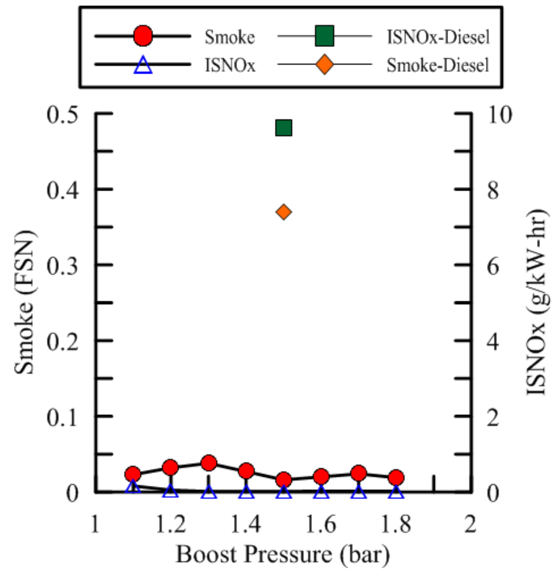

Figure 4.20 ISNOx and smoke emissions at various boost pressures at 5.2 bar IMEP, 80 PES, N= 1500 RPM, Pin = 1.5 bar, injection pressure= 500 bar

The formation of CO depends on the combustion temperature and the mixture homogeneity. There are two main sources that facilitate the formation of CO. Firstly, CO emissions are mainly formed in the low temperature regions such as the boundary layers near cylinder walls. Secondly, CO emissions increase with locally fuel-rich mixture due to lack of oxidation of CO to CO_2. From Figure 4.21 we see that as we increase boost pressure, the ISCO increases. This can be explained by looking at the AHRR plots Figure 4.16 which show that the heat release is highest for 1.1 bar boost pressure case. The bulk in-cylinder temperatures are highest at 1.1 bar boost pressure, thereby aiding the oxidation of CO to CO_2. Also we notice a prominent LTHR slope for 1.8 bar boost pressure, whereas no such LTHR for lower boost pressures. This lower temperature also impedes the complete oxidation of CO. Similar trend is followed by HC since they also increase with decrease in local combustion temperatures.

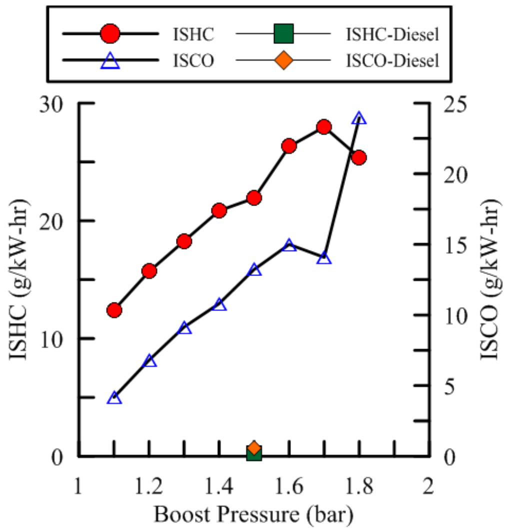

Figure 4.21 ISHC and ISCO emissions at various boost pressures at 5.2 bar IMEP, 80 PES, N= 1500 RPM, Pin = 1.5 bar, injection pressure= 500 bar

CHAPTER V

SUMMARY AND CONCLUSIONS

Diesel-ignited gasoline dual fuel and diesel-ignited methane dual fuel combustion experiments were performed in a single-cylinder research engine (SCRE), outfitted with a common-rail diesel injection system and a stand-alone diesel injection driver. Gasoline was injected in the intake port using a port-fuel injector. Methane was introduced via the intake manifold with the help of a manually controlled needle valve. Parameters such as diesel injection timing, diesel injection pressure, and boost pressure were varied to quantify their impact on engine performance and engine-out ISNOx, ISHC, ISCO, and smoke emissions.Analysis of the results leads to the following conclusions:

5.1 Diesel-Gasoline Dual Fueling

Dual fueling of diesel-gasoline was performed at a constant load of 5.2 bar IMEP at various injection timing, injection pressure and boost pressure conditions.

5.1.1 Injection Timing Sweep

Injection timing sweep was performed by changing diesel injection timing between 30-170 DBTDC. The engine was operated at a constant speed of 1500 rev/min, a constant load of 5.2 bar IMEP, and a constant 80 PES of gasoline. Injection pressure was maintained at 500 bar and intake manifold pressure was set at 1.5 bar, with no EGR.

1. Diesel injection timing (SOI) has a profound influence on diesel-ignited gasoline dual fuel combustion. Advancing SOI from 30 DBTDC to 60 DBTDC reduces ISNOx from 14 g/kWhr to less than 0.1 g/kWhr; further advancement of SOI did not yield significant ISNOx reduction. This is due to a fundamental change in the nature of combustion from heterogeneous combustion at 30 DBTDC to "premixed enough" combustion at 50-80 DBTDC and finally to well-mixed diesel-assisted gasoline HCCI-like combustion at 170 DBTDC. Smoke emissions are less than 0.1 FSN at all SOIs, while ISHC and ISCO are in the range of 8-20 g/kWhr, with the earliest SOIs yielding very high values.
2. Indicated fuel conversion efficiencies are ~ 40-42.5%, and the combustion efficiencies are ~92.5-95.5%. The increasing combustion efficiencies on retarding injection timing directly relate with the lowering of ISHC and ISCO emissions. The highest combustion efficiency is achieved at 70 DBTDC which corresponds to the lowest ISHC and ISCO values of 9 g/kW-hr and 8.4 g/kW-hr respectively.
3. The MPRR increases on advancing the injection timing from 30 DBTDC to 100 DBTDC and reaches 13 bar/CAD. On further advancement of injection timing the MPRR reduces but increases beyond 150 DBTDC. The ignition delay however showed a very uniform trend of increasing linearly with advanced injection timing.
4. CA50 phasing is an important parameter to understand the nature of dual fuel combustion. CA50 phasing was significantly advanced at 30 and 40

DBTDC and phased closer to TDC on advancing the injection timing. This advanced phasing of CA50 at 30 and 40 DBTDC may be one of the reasons behind the high ISNOx emissions due to higher local temperatures for a longer time promoting the formation of thermal NO.

5.1.2 Injection Pressure Sweep

Injection pressure sweep was performed by changing diesel injection pressure between 200-1300 bar. The engine was operated at a constant speed of 1500 rev/min, a constant load of 5.2 bar IMEP, and a constant 80 PES of gasoline. Injection timing was kept constant at 50DBTDC and intake manifold pressure was set at 1.5 bar, with no EGR.

1. An injection pressure sweep from 200 to 1300 bar at 50 DBTDC SOI showed that very low injection pressures led to apparently more heterogeneous combustion and higher ISNOx and ISCO emissions, while smoke and ISHC emissions remain unaffected. An injection pressure of about 500 bar appears to be optimal for early SOIs.
2. Indicated fuel conversion efficiency increases from 39% at 200 bar to 43% at 1300 bar. The CA50 is much more retarded from TDC at 200 bar, and also the CA10-90 duration is longer. The combustion efficiencies however remain unchanged with change in injection pressure.
3. The MPRR increases on increasing the injection pressure, and so does the ignition delay. The increase in ignition delay times is believed to be responsible for very rapid combustion, which in turn leads to high MPRR at 1100 bar and 1300 bar.

5.1.3 Boost Pressure Sweep

A Boost pressure sweep was performed by changing the intake air pressure from 1.1-1.8 bar. The engine was operated at a constant speed of 1500 rev/min, a constant load of 5.2 bar IMEP, and a constant 80 PES of gasoline. Injection pressure was maintained at 500 bar and injection timing was set at 50 DBTDC.

1. A boost pressure sweep from 1.1 to 1.8 bar at 50 DBTDC SOI showed very rapid combustion for the lowest boost conditions (with the highest overall equivalence ratios), leading to high pressure rise rates, higher ISNOx emissions, and lower ISCO emissions due to higher bulk temperatures, while smoke and ISHC emissions remain unaffected by boost pressure.
2. The combustion efficiency remained almost unchanged, while the indicated fuel conversion efficiency increased slightly on increasing boost from 1.1 to 1.3 bar and then started decreasing on further increments in boost. This is likely due to the trends seen in CA5, CA50 and CA10-90. CA5 and CA50 are retarded with decreasing boost which leads to a slight increase in IFCEs.

5.2 Diesel-Methane Dual Fueling

Dual fueling of diesel-methane was performed at a constant load of 5.2 bar IMEP at various injection timing, injection pressure and boost pressure conditions.

5.2.1 Injection Timing Sweep

Injection timing sweep was performed by changing diesel injection timing between 10-110 DBTDC. The engine was operated at a constant speed of 1500 rev/min, a constant load of 5.2 bar IMEP, and a constant 80 PES of methane. Injection pressure was maintained at 500 bar and intake manifold pressure was set at 1.5 bar, with no EGR.

1. Diesel injection timing (SOI) greatly affects the diesel-ignited methane dual fuel combustion. Advancing SOI from 30 DBTDC to 60 DBTDC reduces ISNOx from 12 g/kW-hr to less than 0.02 g/kW-hr; further advancement of SOI did not yield significant ISNOx reduction. This is due to a fundamental change in the nature of combustion from heterogeneous combustion at and before 30 DBTDC to "premixed enough" combustion at 50-80 DBTDC and finally to well-mixed diesel-assisted homogenous charge combustion at 110 DBTDC. Also the the injection timing is advanced beyond 30 DBTDC, the heat release rate reduces thereby lowering local in-cylinder temperatures and ISNOx. Smoke emissions are less than 0.1 FSN at all SOIs. ISHC and ISCO are very high at close to TDC timings (e.g., 49 g/kW-hr at 10 DBTDC) but decrease to a value of 17 g/kW-hr on advancing timing to 80 DBTDC, beyond that ISHC again starts to increase. ISCO increases from 7.3 g/kW-hr at 50 DBTDC to 25 g/kW-hr at 110 DBTDC.
2. Indicated fuel conversion efficiency increases from 28% at 10 DBTDC to 35.4% at 60 DBTDC. This is likely due to increased combustion efficiency. The combustion efficiency trend is also consistent with the

trend observed with ISHC and ISCO. The lower the combustion efficiency at very retarded (10-20 DBTDC) and very advanced (90-110 DBTDC) injection timing, the higher the ISHC and ISCO emissions, and vice versa.

3. The MPRR increases from 10-30 DBTDC attaining 10.4bar/CAD for SOI of 30 DBTDC and then decreases continuously on further advancement of injection timing. The ignition delay continues to increase on advancing injection timing primarily due to increased residence times available for the mixing of diesel in the methane-air mixture.
4. The premixed combustion which may be taking place between 20-40 DBTDC range is responsible for the shift in CA50 from ATDC to BTDC, but then again it shifts to ATDC on further advancements in injection timing due to "well mixed" conditions beyond 50 DBTDC.

5.2.2 Injection Pressure Sweep

Injection pressure sweep was performed by changing diesel injection pressure between 200-1300 bar. The engine was operated at a constant speed of 1500 rev/min, a constant load of 5.2 bar IMEP, and a constant 80 PES of methane. Injection timing was kept constant at 60DBTDC and intake manifold pressure was set at 1.5 bar, with no EGR.

1. An injection pressure sweep from 200 to 1300 bar at 60 DBTDC SOI showed that very low injection pressures lead to apparently more heterogeneous combustion and higher ISNOx and ISHC emissions. ISCO increased on increasing injection pressures, while smoke remained unaffected. An injection pressure of about 500 bar appears to be optimal for early SOIs.

2. Indicated fuel conversion efficiency and combustion efficiency remain unaffected by change in injection pressures. CA 50 is phased closer to TDC at higher injection pressures.
3. MPRR decreases with increases in injection pressure. The maximum value of MPRR noticed was 6.1 bar/CAD at 200 bar injection pressure. The ignition delay increases linearly with increase in injection pressure.

5.2.3 Boost Pressure Sweep

A Boost pressure sweep was performed by changing the intake air pressure from 1.1-1.8 bar. The engine was operated at a constant speed of 1500 rev/min, a constant load of 5.2 bar IMEP, and a constant 80 PES of methane. Injection pressure was maintained at 500 bar and injection timing was set at 60 DBTDC.

1. Increase in boost pressure did not affect ISNOx and smoke too much. They remained fairly low at all boost conditions (ISNOx < 0.15 g/kW-hr; Smoke < 0.1 FSN). However, increasing boost pressure did increase both ISHC and ISCO emissions, which may be due to decrease in in-cylinder temperatures caused by the excess air, preventing the complete oxidation of CO and leaving behind unburnt HC. Also the increase in HC at higher boost conditions may be due to the increase in the mass of HC trapped in crevices due to increased cylinder pressures and boost pressures.
2. Indicated fuel conversion efficiency remained unaltered, but the combustion efficiency decreased from 92% at 1.1 bar boost pressure, to 84% at 1.8 bar boost. This decrease in combustion efficiency also suggests

an attendant increase in ISHC and ISCO at higher boost conditions. CA50 is continuously retarded on increasing boost pressure conditions.

3. MPRR increases with increase in boost pressure. Ignition delay decreases with increase in boost pressure. The lower ignition delay periods are the primary reason for increased MPRR conditions at higher boost pressure conditions.

CHAPTER VI

COMPARISON

Table 6.1 Diesel-Gasoline VS. Diesel-Methane Dual Fueling

Parameters	Diesel-Gasoline	Diesel-Methane
MPRR	Decreases from 30-40DBTDC and then steadily increases upto a value of ~13bar/CAD at 100 DBTDC. On further advancement of SOI the MPRR decreases slightly till 150 DBTDC after which it again increases to 13 bar/CAD at 170 DBTDC	Increases from 10-30 DBTDC and reaches a maximum value of ~ 10 bar/CAD. On further advancement in injection timing the MPRR continues to decrease and becomes nearly constant beyond 90DBTDC.
Ignition Delay	Increases linearly from 30-170 DBTDC (14 CAD or 1.55 ms to 165.3 CAD or 18.36 ms)	Fairly constant between 10-20 DBTDC (9.4 CAD or 1.04 ms to 9.8 CAD or 1.08 ms and increases linearly from 30-110 DBTDC (13.4 CAD or 1.48 ms to 110.2 CAD or 12.24 ms.
CA50	Phased closer to TDC on increasing injection timing, but remains in the BTDC region throughout. Ranges from 350 CAD to 358 CAD	Shifts from ATDC to BTDC on increasing injection timing from 10-30 DBTDC. On further advancement CA50 starts decreasing and shifts back to ATDC. Ranges between 350 CAD and 371 CAD
CA5	Phases from 344 CAD at 30DBTDC SOI to nearly 356 CAD at 170 DBTDC SOI	Phased at TDC for 10 DBTDC SOI and continues to advance to nearly 345 CAD for SOI of 40 DBTDC. On further advancement of SOI CA5 moves closer to TDC and reaches TDC again at 110 DBTDC SOI

Table 6.1 (Continued)

CA10-90	Decreases from 12 CAD (1.33 ms) to 6 CAD (0.67 ms) on increasing injection timing from 30-170DBTDC	Decreases from 23 CAD (2.55 ms) at 10 DBTDC to 13 CAD (1.44 ms) at 50 DBTDC. It remains fairly constant between 50-110 DBTDC SOI
Combustion Efficiency	Decreases with injection advance. However remains between 92-95%	Increases with injection advance from 20-60 DBTDC. Reaches 85% at 60 DBTDC. On further advancing again drops down to 76% for 110 DBTDC injection timing.
Indicated Fuel Conversion Efficiency	Remains fairly constant fluctuating between 40-42% for all injection timings	Increases from 28-35% on advancing from 10-60 DBTDC. Advancing further leads to a gradual drop to 31.6% at 110 DBTDC
COV_{IMEP}	Remains constant at nearly 1.5 for the complete injection timing range	Decreases from 4 to 1.7 between 10-30 DBTDC SOI, and then increases to 13 at 110 DBTDC.
ISHC	Decreases from 10 g/kW-hr at 30 DBTDC to about 9 g/kW-hr at 60 DBTDC and then increases to nearly 14 g/kW-hr at 170 DBTDC.	Decreases from 84 g/kW-hr at 10 DBTDC to 33 g/kW-hr at 60 DBTDC and then increases to 60 g/kW-hr at 110 DBTDC
ISNOx	On increasing from 30-40 DBTDC the NOx emissions drop from 14 g/kW-hr to 2 g/kW-hr and on further SOI advance bring down NOx emissions to near zero levels	NOx emissions increase from 3.8 g/kW-hr at 10 DBTDC to 14 g/kW-hr at 30 DBTDC, and dramatically drops to 2.3 g/kW-hr at 40 DBTDC. On futher advance the NOx emissions reach near zero values
Smoke	Smoke remains unchanged and very low (under 0.1 FSN)	Smoke remains unchanged and very low (under 0.1 FSN)

CHAPTER VII

RECOMMENDATIONS FOR FUTURE WORK

1. Operate engine at higher load conditions (up to 10 bar BMEP) for both diesel-gasoline and diesel-methane cases, results of which would be of profound interest to the commercial sector.

2. Install and use an EGR system on the Single Cylinder Research Engine setup so as to operate at higher loads. Additionally, the EGR effects on NOx, PM and fuel conversion efficiencies should be investigated.

3. Compare the current dual fueling cases of diesel –gasoline and diesel-methane with some other interesting dual fuel cases such as diesel-propane and diesel-E85.

4. Analysis of particle size distribution with the help of engine exhaust emissions particle sizer for high and low-load conditions for both diesel-gasoline and diesel-methane would be something worth looking into as many studies are being published every day about the health hazards due to the fine suspended particles in the air. One of the major sources of such fine particulate emissions is the transportation sector, and thus it is important to start looking into it.

5. Very high boost conditions of 2.5-3 bar with the dual fueling cases could also be an interesting study to do. It may help in going up to higher load and more lean and efficient engine running conditions.

REFERENCES

Agarwal, A. K., 2007, "Biofuels (alcohols and biodiesel) applications as fuels for internal combustion engines," *Prog. Energy Combust Sci.*, 33, 233–271.

Anderson, R.W., and Lim, M. T.,1985, "Investigation of misfire in a fast burn Spark Ignition Engine," Combustion Science and Technology, Vol. 43, p. 915.

Chao, Y., Jian-xin, W. , Zhi, W., and Shi-jin, S., 2013, "Comparative study on Gasoline Homogeneous Charge Induced Ignition (HCII) by diesel and Gasoline/Diesel Blend Fuels (GDBF) combustion," *Fuel*, 106, pp. 470-477.

Cheng, A. S., Fisher, B. T., Martin, G. C., Mueller, C. J., 2010,"Effects of Fuel Volatility on Early Direct-Injection, Low-Temperature Combustion in an Optical Diesel Engine," *Energy and Fuels, 24, pp.1538-1551*

Ciatti, S.A., and Subramanian, S., 2011, "An Experimental Investigation of Low-Octane Gasoline in Diesel Engines," *ASME Journal of Engineering for Gas Turbines and Power*, 133(9), 092802 doi:10.1115/1.4002915.

Combustion, I. Glassman, 3rd. ed., 1996, Academic Press, London, U.K.

Czerwinski, J., 1994 "Performance of HD-DI diesel engine with addition of ethanol and rapeseed oil," SAE paper No. 940545.

Dec, J.E., (2009) "Advanced Compression-Ignition Engines – Understanding The In-Cylinder Processes." *Proceedings of the Combustion Institute*, 32, 2727-2742.

Dorado, M. P., Ballesteros, E., Arnal, J. M., Gomez, J., and Lopez, F. J., 2003, **"**Exhaust emissions from a diesel engine fueled with transesterified waste olive oil," *Fuel*, 82(11), 1311–1315.

Doughty, G. E., Bell, S. R. and Midkiff, K. C.,1992, "Methane Fueling of a Caterpillar 3406 Diesel Engine," *J. Eng. Gas Turbines Power* 114(3), pp. 459-465

Fruin, S.A., St. Denis, M. J., Winer, A. M., Colome, S. D., Lurmann, and F. W., 2001, " Reductions in human benzene exposure in the California South Coast Air Basin," *Atmospheric Environment*, 35(6), pp. 1069–1077.

Han, D., Ickes, A. M., Bohac, S. V., Huang, and Z., Assanis, D. N., 2011, "Premixed low-temperature combustion of blends of diesel and gasoline in a high speed compression ignition engine," *Proceedings of the Combustion Institute*, 33(2), pp. 3039-3046.

Han, D., Ickes, A. M., Bohac, S. V., Huang, Z., Assanis, and D. N., 2012, "HC and CO emissions of premixed low-temperature combustion fueled by blends of diesel and gasoline," *Fuel*, 99, 13-19.

Hanson, R., Splitter, D., and Reitz, R., 2009, "Operating a Heavy-Duty Direct-Injection Compression-Ignition Engine with Gasoline for Low Emissions", SAE Paper No. 2009 -01-1442.

Heywood, J.B., 1998, "Internal Combustion Engine Fundamentals," McGraw Hill, Inc.

Inagaki, K., Fuyuto, T., Nishikawa, K., and Nakakita, K., and Sakata, I., 2006, "Dual-fuel PCI combustion controlled by in-cylinder stratification of ignitability," SAE Paper No. 2006-01-0028.

Kalghatgi G. T., Gurubaran, R. K., Davenport, A., Harrison, A. J., Hardalupas, Y., and Taylor, A. M. K. P., 2013, "Some advantages and challenges of running a Euro IV, V6 diesel engine on a gasoline fuel," *Fuel*, 108, 197-207.

Kalghatgi, G. T., Risberg, P., and Angstrom, H., 2007, "Partially pre-mixed auto-ignition of gasoline to attain low smoke and low NOx at high load in a compression ignition engine and comparison with a diesel fuel," SAE Paper No. 2007-01-0006.

Kalghatgi, G., Hildingsson, L., and Johansson, B., 2009, "Low NOx and low smoke operation of a diesel engine using gasoline-like fuels", Proceedings of the ASME Internal Combustion Engine Division 2009 Technical Conference, ICES2009-76034.

Kalghatgi, G.T., Hildingsson, L., Harrison, A. and Johansson, B., 2010, "Low-NOx, low-smoke operation of a diesel engine using "premixed enough" compression ignition - Effects of fuel autoignition quality, volatility and aromatic content," presented at THIESEL 2010 Conference on Thermo- and Fluid Dynamic Processes in Diesel Engines.

Kalghatgi, G.T., Hildingsson, L., Harrison, A.J., Johansson, B., 2011, "Autoignition quality of gasoline fuels in partially premixed combustion in diesel engines," *Proceedings of the Combustion Institute*, 33, 3015–3021.

Karabektas, M., Ergen, G., and Hosoz, M., 2011, "Effects of the blends containing low ratios of alternative fuels on the performance and emission characteristics of a diesel engine," *Fuel*, In Press, Corrected Proof, Available online 8 May 2011, http://dx.doi.org/10.1016/j.fuel.2011.04.036.

Karim,G.A., 2003,“Combustion in Gas Fueled Compression Ignition Engines of the Dual Fuel Type” Transaction of the ASME: Journal of Engineering for Gas Turbines and Power, Vol. 125, pp. 827-836

Kokjohn, S. L., Hanson, R. M., Splitter, D. A., and Reitz, R. D., 2009 “Experiments and Modeling of Dual-Fuel HCCI and PCCI Combustion Using In-Cylinder Fuel Blending,” SAE Int. J. Engines, Paper No. 2009-01-2647.

Kokjohn, S. L., Hanson, R. M., Splitter, D. A., and Reitz, R. D., 2011, “Fuel reactivity controlled compression ignition (RCCI): a pathway to controlled high-efficiency clean combustion,” *International Journal of Engine Research*, 12(3), pp. 209-226.

Krishnan, S. R., Srinivasan, K. K., Singh, S., Bell, S. R., Midkiff, K.C., Gong, W., Fiveland, S.B., and Willi, M., 2004, “Strategies for Reduced NOx Emissions in Pilot-Ignited Methane Engines,” *Journal of Engineering for Gas Turbines and Power*, Vol. 126, Issue 3, pp.665-671

Krishnan, S.R., and Srinivasan, K.K., 2010,“Multi-zone modelling of partially premixed low-temperature combustion in pilot-ignited natural-gas engines,” Proc. IMechE, Part D: J. Automobile Engineering, 224(D12), pp. 1597-1622.

Lin, Y., Wu, Y. G., and Chang, C. T., 2007, “Combustion characteristics of waste-oil produced biodiesel/diesel fuel blends,” *Fuel*, 86(12-13), 1772–1780.

Manente, V., Johansson, B., Tunestal, P., and Cannella, W., 2010, “Influence of inlet pressure, EGR, combustion phasing, speed and pilot ratio on high load gasoline partially premixed combustion,” SAE Paper No. 2010-01-1471.

Manente, V., Tunestal, P., and Johansson, B., 2009, “Partially premixed combustion at high load using gasoline and ethanol, a comparison with diesel,” SAE Paper No. 2009-01-0944.

Marshall, J. D., Riley, W. J., McKone, T. E., Nazaroff, and W. W., 2003, “Intake fraction of primary pollutants: motor vehicle emissions in the South Coast Air Basin,” *Atmospheric Environment*, 37(24), pp. 3455–3468.

Martin, G., Mueller, C., Milam, D., Radovanovic, M., Gehrke, C., 2008, “Early Direct-Injection, Low-Temperature Combustion of Diesel Fuel in an Optical Engine Utilizing a 15-Hole, Dual-Row, Narrow-Included-Angle Nozzle,” SAE Paper No. 2008-01-2400

Mysliwiec, M. J., Kleeman, and M. J., 2002, “Source apportionment of secondary airborne particulate matter in a polluted atmosphere,” *Environmental Science & Technology*, 36(24), pp. 5376–5384.

Papagiannakis, R. G., and Hountalas, D. T.,2004,“Combustion and exhaust emission characteristics of a dual fuel compression ignition engine operated with pilot diesel fuel and methane” Energy Conversion and Management, 45 (18/19) (2004), pp. 2971–2987

Pitt, P. L., 1984,“An Ignition system for ultra lean mixtures” Combustion Science and Technology, Vol. 35, pp. 277-285

Polk, A. C., Dwivedi, U., Carpenter, C. D., Guerry, E. S., Srinivasan, K. K., and Krishnan, S. R., 2013,“Diesel-ignited propane dual fuel LTC in a heavy-duty diesel engine” ASME Conference, 2013

Qi. Y, Srinivasan, K. K., Krishnan, S. R.,Yang, H., Midkiff, K. C., 2007 "Effect of hot EGR on the performance and emissions of an advanced injection low pilot-ignited methane engine," *International Journal of Engine Research*, Vol. 8, No. 3, pp. 289-305

Quader, A.A., 1974,“Lean combustion and the misfire limit in spark ignition engine,” SAE Paper No. 741055.

Rogge, W. F., Hildemann, L. M., Mazurek, M. A., Cass, G. R., Simoneit, and B. R. T., 1993, “Sources of fine organic aerosol 2: noncatalyst and catalyst-equipped automobiles and heavy-duty diesel trucks,” *Environmental Science & Technology*, 27(4) , pp. 636–651.

Sayin, C., 2010, “Engine performance and exhaust gas emissions of methanol and ethanol–diesel blends,” *Fuel*, 89(11), 3410–3415.

Siebers, D. L., 1999, “Scaling liquid-phase fuel penetration in diesel sprays based on mixing-limited vaporization,” SAE 1999-01-0528.

Splitter, D. A., Hanson, R. M., Kokjohn, S. L., and Reitz, R. D., 2011, “Reactivity controlled compression ignition (RCCI) engine operation at mid and high loads with conventional and alternative fuels,” SAE Paper No. 2011-01-0363.

Srinivasan, K. K., Krishnan, S. R., Midkiff, K. C., 2006 “Improving low load combustion, stability and emissions in pilot-ignited methane engines,” *Proc. Instn. Mech.Engrs.: Journal of Automobile Engineering*, Part D, 220(2), pp. 229-239.

Srinivasan, K. K., Krishnan, S. R., Singh, S., Midkiff, K.C., Bell, S.R., Gong, W., Fiveland, S. B., and Willi, M., 2006, “The Advanced Low Pilot Ignited Methane Engine – A Combustion Analysis,” *Journal of Engineering for Gas Turbines and Power*, Vol. 128, Issue 1., pp. 213-218

Srinivasan, K.K., Krishnan, S. R., Qi, Y., Yang, H., Midkiff, K.C., 2007 "Analysis of diesel pilot-ignited methane low-temperature combustion with hot exhaust gas recirculation," *Combustion Science and Technology*, 179(9), pp. 1737-1776.

Weall, A.J., and Collings, N., 2009, "Gasoline Fuelled Partially Premixed Compression Ignition in a Light Duty Multi Cylinder Engine: A Study of Low Load and Low Speed Operation," SAE Paper No. 2009-01-1791.